Since January 2020 Elsevier has created a COVID-19 resource centre with free information in English and Mandarin on the novel coronavirus COVID-19. The COVID-19 resource centre is hosted on Elsevier Connect, the company's public news and information website.

Computers in Biology and Medicine 150 (2022) 106134

Contents lists available at ScienceDirect

Computers in Biology and Medicine

journal homepage: www.elsevier.com/locate/compbiomed

Analysis and identification of potential type II helper T cell (Th2)-Related key genes and therapeutic agents for COVID-19

Qiying Jin [a], Wanxi Li [a], Wendi Yu [a], Maosen Zeng [a], Jinyuan Liu [b], Peiping Xu [a,*]

[a] Institute of Tropical Medicine, Guangzhou University of Chinese Medicine, Guangzhou, PR China
[b] Basic Medical College, Guangzhou University of Chinese Medicine, Guangzhou, PR China

ARTICLE INFO

Keywords:
COVID-19
Type II helper T cell (Th2)
Key genes
Therapeutic agents

ABSTRACT

COVID-19 pandemic poses a severe threat to public health. However, so far, there are no effective drugs for COVID-19. Transcriptomic changes and key genes related to Th2 cells in COVID-19 have not been reported. These genes play an important role in host interactions with SARS-COV-2 and may be used as promising target. We analyzed five COVID-19-associated GEO datasets (GSE157103, GSE152641, GSE171110, GSE152418, and GSE179627) using the xCell algorithm and weighted gene co-expression network analysis (WGCNA). Results showed that 5 closely correlated modular genes to COVID-19 and Th2 cell enrichment levels, including purple, blue, pink, tan and turquoise, were intersected with differentially expressed genes (DEGs) and 648 shared genes were obtained. GO and KEGG pathway enrichment analyses revealed that they were enriched in cell proliferation, differentiation, and immune responses after virus infection. The most significantly enriched pathway involved the regulation of viral life cycle. Three key genes, namely CCNB1, BUB1, and UBE2C, may clarify the pathogenesis of COVID-19 associated with Th2 cells. 11 drug candidates were identified that could down-regulate three key genes using the cMAP database and demonstrated strong drugs binding energies aganist the three keygenes using molecular docking methods. BUB1, CCNB1 and UBE2C were identified key genes for COVID-19 and could be promising therapeutic targets.

1. Introduction

Coronavirus disease 2019 (COVID-19) is a viral pneumonia caused by severe acute respiratory syndrome coronavirus 2 (SARS-Cov-2) [1]. The main symptoms of SARS-Cov-2 infection are fever, loss of taste or smell, cough, shortness of breath, severe pneumonia and acute respiratory distress syndrome [2]. At present, several effective SARS-Cov-2 vaccines and antiviral drugs (e.g. Remdesivir and Nirmatrelvir) provide for some control of the viral infection and associated symptoms [3–5]. However, due to the variability, mutation and genetic drift of the virus, SARS-Cov-2 has persisted even with mass immunization and vaccination. As such, the COVID-19 epidemic continues [6]. Moreover, adverse reactions have been reported, e.g. vaccine related complications and drug toxicities [7,8]. Therefore, it is still an urgent need to explore more effective means by which to fight the virus, reducing incidence and side effects. Unfortunately, the molecular basis for SARS-CoV-2 infection and the interaction of the virus with the host have not been fully elucidated, limiting the development of therapeutic drugs for COVID-19. Therefore, it is essential to explore the biology of SARS-CoV-2 infection, evaluate the host response to infection, identify effective therapeutic targets at the molecular/immunological level, and develop new therapeutic strategies for COVID-19 [9].

Since the outbreak of COVID-19, many studies have been conducted to understand the molecular mechanisms and host-pathogen interactions associated with COVID-19 by analyzing viral gene expression in various tissues of COVID-19 patients [10]. For example, functional genomics were evaluated for bronchoalveolar lavage fluid and peripheral blood mononuclear cells (PBMC) based on microarray and RNA sequencing analysis [11,12]. Meanwhile, bioinformatics tools including biomarkers, network analysis, and characteristic gene recognition have been used to identify and establish molecular markers for different diseases [13–15]. These tools have been widely used for the study of COVID-19 biomarkers and as well for the identification of potential targets for treatment [1,16]. Studies have reported some COVID-19 hub genes including ICAM1, RBX1, PTEN, VPS29, TXN, CANX, PSMC2, REEP5, ACTR2, TNFSF13B, ARPC3, HSP90AA1, MAPK1, LCN2, STAT1, UBE2L6, and MX1 [17–28]. However, COVID-19 transcriptomic

* Corresponding author. Institute of Tropical Medicine, Guangzhou University of Chinese Medicine, 12 Jichang Rd., San Yuanli St., Bai Yun Dist., Guangzhou, 510405, Guangdong, PR China.
E-mail address: xupeiping@gzucm.edu.cn (P. Xu).

https://doi.org/10.1016/j.compbiomed.2022.106134
Received 19 March 2022; Received in revised form 30 August 2022; Accepted 18 September 2022
Available online 22 September 2022

Abbreviations

Th2	type II helper T cell
COVID-19	coronavirus disease 2019
SARS-Cov-2	severe acute respiratory syndrome coronavirus 2
Th1	typeIhelper T cell
IL	interleukin
WGCNA	weighted gene coexpression network analysis
GS	gene significance
MM	module membership
GO	gene ontology
KEGG	Kyoto encyclopedia of genes and genomes
PPI	protein-protein interaction
DEGs	differentially expressed genes
ROC	receiver operating characteristic
ANOVA	Analysis of variance
UBE2C	ubiquitin-conjugating enzyme E2C
CCNB1	cyclin B1
BUB1	budding uninhibited by benzimidazoles 1
AUC	area under curve
FC	fold change
BP	biological process
CC	cellular composition
MF	molecular function

changes during disease and the key genes important to type II helper T cells (Th2) during infection have not been reported. These genes likely play an important role in host and SARS-CoV-2 interaction, and as such may be promising targets for drug treatment.

Weighted gene coexpression network analysis (WGCNA) is a system biology method, which identifies highly related gene clusters (modules), candidate biomarkers and therapeutic targets for various diseases, including viruses [17,29,30]. The combination of high-throughput technology and WGCNA provide a new opportunity to better understand the molecular basis for COVID-19 and other infectious diseases [31,32].

Previous studies have shown that the main cause of death from SARS-CoV-2 infection is a result of excessive inflammation. Proinflammatory cytokines such as interleukin (IL)-6, IL-1α/β, tumor necrosis factor (TNF)-α, IL-8, and monocyte chemoattractant protein (MCP)-1 promote disease severity and tissue damage in patients with COVID-19 [33,34]. The massive release of cytokines and chemokines leads to excessive inflammation and immune cell mobilization, resulting in the so-called "cytokine storm" pathological phenomenon [35]. It is worth noting that SARS-CoV-2 infection can increase the secretion of Th2-induced cytokines (e.g.IL-13 and IL-4) into plasma [2]. Th1/Th2 imbalance can lead to chronic infection and a poor prognosis for COVID-19 patients [36,37]. Therefore, identification of potential biomarkers related to Th2 cell during COVID-19 infection may explain the course of COVID-19 infection, deepen understanding of the molecular basis for SARS-CoV-2 infection, and improve diagnosis and treatment for COVID-19.

Herein, the COVID-19 related gene expression data sets (GSE157103, GSE152641, GSE171110, GSE152418, and GSE179627) were studied. The xCell algorithm [38] was employed to enrich Th2 related gene expression data. WGCNA was used to construct gene co-expression network modules closely related to disease traits. Then, relevant modules were screened to obtain important genes closely related to COVID-19 and Th2 cells. The gene ontology (GO) and Kyoto encyclopedia of genes and genomes (KEGG) databases were used to analyze the biological function and pathway enrichment of the shared genes after the intersection of WGCNA related modules and differentially expressed genes (DEGs). A protein-protein interaction (PPI) network was established and cytoHubba was used to identify the hub genes associated with Th2 cells during COVID-19 infection of patients. Receiver operating characteristic (ROC) and other validation datasets were used to identify and validate the identified hub genes. A connectivity map (cMAP) database was used to identify small molecules or drugs that may affect key genes of Th2 lymphocytes during COVID-19 infection. Finally, the molecular docking simulation was implemented to analyze the drugs binding energies aganist the three keygenes.

2. Materials and methods

2.1. COVID-19 microarray datasets

GSE157103, GSE152641, GSE171110, GSE152418, and GSE179627 microarray data were downloaded from the gene expression omnibus (GEO) database (http://www.ncbi.nlm.nih.gov/geo/). The information of the five datasets were summarized in Table 1. We further paired the GSE157103 and GSE152641 as a discovery cohort for the WGCNA analysis, and GSE171110, GSE152418, and GSE179627 were used for validation set. The datasets were eventually batch-normalized using the R packages "sva" and "limma" [39]. DEGs in the discovery cohort were identified by "limma" R package [logFC (fold-change) values = 0.5, *p*-values = 0.05].

2.2. Estimation of extent of immune cell enumeration in COVID-19

In this study, we applied the xCell algorithm to determine the immune cell subsets in the discovery set (GSE157103 and GSE152641) [40]. The xCell algorithm is a gene signatures-based method learned from thousands of pure cell types from various sources and can performs cell type enumeration analysis from gene expression data for 64 immune and stroma cell types, which makes it an excellent tool for reliably portraying the cellular heterogeneity landscape of tissue expression profiles [38].

2.3. Establishment and identification of Co-expression networks

We used the WGCNA to obtain the COVID-19 and Th2 cell associated modules. About 15,385 genes that were expressed in 162 COVID-19 samples. About 4488 genes were used to perform WGCNA analysis. The main parameters were as follows: variance of selected genes >25%, cutHeight = 85, soft threshold (power) = 0.8, minModuleSize = 60, MEDissThres = 0.2. Pearson's test was used to calculate the correlation between COVID-19 and Th2 cell enrichment levels and modules. The modules with large correlation coefficient between COVID-19 and Th2 cell subsets and p values < 0.05 were included in the next study.

2.4. Analysis of GO, KEGG and PPI enrichment

The R software package 'VennDiagram' was used to intersect the genes in the meaningful modules obtained from WGCNA analysis with DEGs. The obtained intersection genes (*i.e.* shared genes) were analyzed by PPI, GO and KEGG. The KOBAS-i (version 3.0, http://kobas.cbi.pku.edu.cn/) was used to carry out KEGG enrichment analysis [41]. Using David database (https://david.ncifcrf.gov/tools.jsp) to perform GO annotation and enrichment analysis, including biological process (BP), cellular component (CC) and molecular function (MF) [42,43]. Select the adjusted *P* value of 0.05 as the standard to determine the enrichment item. STRING database (https://string-db.org/) was used to performe

Table 1
Summary of five GEO datasets involving COVID-19 patients.

ID	GSE number	Platform	Samples	Source types	Disease	Group
1	GSE157103	GPL24676	100 patients and 26 controls	Leukocytes from whole blood	COVID-19	Discovery set
2	GSE152641	GPL24676	62 patients and 24 controls	Whole blood	COVID-19	Discovery set
3	GSE171110	GPL16791	54 patients and 10 controls	Peripheral blood	COVID-19	Validation set
4	GSE152418	GPL24676	17 patients and 17 controls	PBMC	COVID-19	Validation set
5	GSE179627	GPL24676	22 patients and 48 controls	PBMC	COVID-19	Validation set

PPI network analysis (confidence = 0.990) and explore the interactions among proteins [44].

2.5. Identification of hub genes in PPI networks of shared genes

CytoHubba is a plug-in of Cytoscape software, which can be used to explore important nodes of biological networks [45]. In this study, Cytoscape 3.8.2 was adopted to visualize the module network, and cytoHubba was used to analyze the network [46]. Then, the maximum clique centrality (MCC) algorithm of cytoHubba was selected to determine the top 20 genes with the highest scores in important modules as hub genes.

2.6. Identification and validation of key genes of COVID-19

Key genes were identified by DEGs and ROC analysis. The differences of gene expression of 20 hub genes were verified in the validation set. At the same time, the R software package 'pROC' was used to assess hub genes in the discovery and validation set.

2.7. Screening potential therapeutic agents for COVID-19

The cMAP database (Broad Institutes, https://www.broadinstitute.org/connectivity-map-cmap) [47] was used to predict the possible small molecules or drugs with high FC value that down-regulate the gene expression of key genes may be potentially therapeutic for COVID-19. PubChem (https://pubchem.ncbi.nml.gov) was used to obtain the detailed information of the potential therapeutic agents.

2.8. Molecular docking analysis

Three key proteins involved in viral infection and replication were considered as potential drug targets. The molecular docking simulations were carried out using the method of AutoDock Vina [48]. Protein crystal structures including CCNB1 (PDB: 6GU2), BUB1 (PDB: 6FTB), and UBE2C (PDB:1I7K) were obtained from PDB database (https://www.rcsb.org/pdb) in pdb format. The structures of 11 drugs predicted to down-regulate 3 key genes from the cMAP database were obtained from the PubChem database (https://pubchem.ncbi.nlm.nih.gov/) in sdf format. Proteins and drugs were prepared by AutoDockTools (v1.5.6). The molecular graphics were prepared by PyMOL (v2.3) [49]. All hydrogens and gasteriger charges were added to each molecule. Docking areas and AutoGrid parameters were set based on the binding pockets of proteins. Ligplot^{+} v2.2 was used to analyze the interaction between protein and ligand [50].

2.9. Statistical analysis

All bioinformatics analysis were carried out using R 4.0.3 software or Perl. GraphPad Prism 5.0 (GraphPad Software Inc., San Diego, CA, USA) was used to draw ROC curve and merge plots. Statistical analysis was performed using version 18.0 (SPSS, Chicago, IL, USA). Analysis of variance (ANOVA) was used to compare the multiple gene expression among COVID-19 patients with different disease degrees. $p < 0.05$ was considered to be statistically significant.

3. Results

3.1. Gene expression omnibus (GEO) information

The mRNA expression profiles of 162 pairs of COVID-19 and 50 control samples in the discovery set (GSE157103 and GSE152641) were merged and batch-normalized for the following analysis (Table 1). We selected genes with differential analysis (adj. $p < 0.05$ and $|\log 2\ FC| > 0.5$) between control and COVID-19 tissues to serve as DESs. The heatmap and volcano plot showed the distribution of genes expressed between COVID-19 and control tissue (Fig. 1). Top 60 up-regulated and down-regulated genes DEGs included TUBB2A, HBB, SLC25A39, HBA2, HBA1, PDZK1IP1, SELENBP1, MYL4, VMO1, LYPD2, TPPP3, CDKN1C, FCER1A, CACNG6, PRSS33, PTGDR2, CLEC10A, PID1, SHISA4, CRIP2, SPNS3, PLD4, MAL, CD7, STMN3, RPLP2, CCL3L1, TTC9, ID3, FCER2, SERPING1, OAS3, IFIT3, IFIT1, IFI44, IFI44L, CMPK2, PSAD2, OASL, EPSTI1, LY6E, IFI27, OTOF, USP18, SIGLEC1, SDC1, TNFRSF17, JCHAIN, TXNDC5, MZB1, TYMS, CDK1, RRM2, OLAA, DEFA3, DEFA4, LTF, CEACAM8, OLFM4, and MMP8.

3.2. Estimation of the immune-enumeration level in COVID-19

xCell algorithm analyzes the enumeration of the 64 immune and stroma cell types in 212 samples (Fig. 2,Supplementary Table S1). There were significant difference in the enrichment fraction of basophils, DC, endothelial cells, MEP, MSC, macrophages, macrophages M1, megakaryocytes, cardiomyocytes, NK cells, NKT, plasma cells, platelets, smooth muscle, Th1 cells, and Th2 cells between the two groups ($p < 0.05$–0.001). The enrichment fraction of Th2 cells in COVID-19 group was significantly higher than that in the control group ($p < 0.001$). Therefore, the enrichment level of Th2 cells in COVID-19 samples were selected as the trait characteristic data of WGCNA.

3.3. Construction of the Co-expression network related to COVID-19 and Th2 cells using WGCNA

In this study, 212 samples and 4488 genes were analyzed by WGCNA. Taking COVID-19 and Th2 cell enrichment scores as disease traits, the module trait relationship heatmap was drawn to evaluate the relationship between each module and clinical traits.

Genes were selected to construct the gene coexpression network according to scale-free criteria $\beta = 0.8$ ($R^2 = 0.80$)(Fig. 3A). Then, a hierarchical clustering tree was established, and the gene modules were identified by dynamic tree cutting method. The minimum number of genes in each module was set to 60. Similar expression modules were combined to obtain 12 modules (Fig. 3B). As shown in Fig. 3C, the correlation of blue, pin, purple, tan, and turquoise modules between COVID-19 and Th2 cells were greater than that of other modules, which were statistically significant ($p < 0.05$). Especially, the highest positive correlation between COVID-19 and Th2 cells was pink module (cor = 0.82,$p < 0.001$) (Fig. 3D). Ultimately, these five modules were selected for further research.

3.4. Identification of shared genes

Five closely correlated and statistically significant module genes

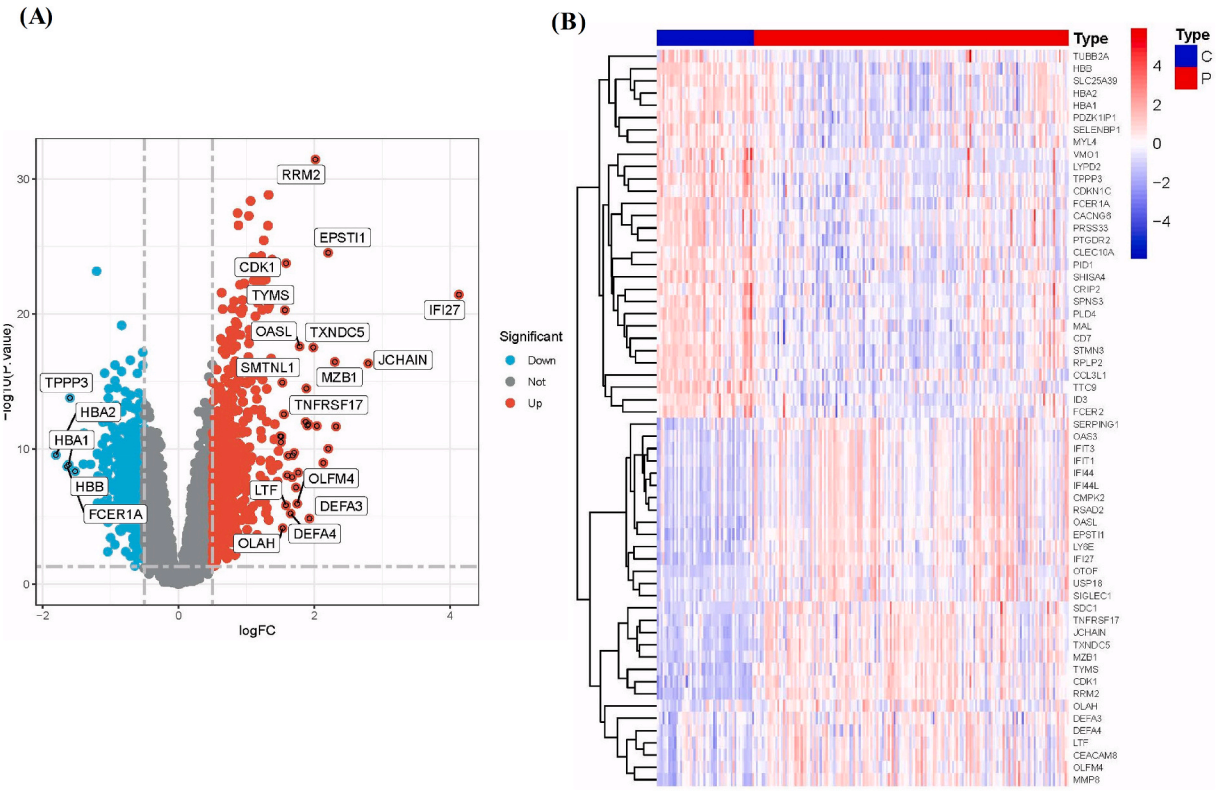

Fig. 1. Volcano and heatmap map of genes differentially expressed between COVID-19 and control samples.
(A) Volcano map of DEGs. (B) Heatmap of top 60 up-regulated and down-regulated genes DEGs. Blue dots represent control samples and pink dots represent COVID-19 samples. red or sapphire blue dots represent genes that were significantly upregulated or down-regulated, respectively. The X axis represents the corrected p-value (scale conversion using logarithm), and the Y axis represents the fold change (logFC). Each dot in the figure represents a gene; red or cyan dots represent genes that were significantly up-regulated or downregulated, respectively, and grey dots represent genes that have no difference in expression between control samples and COVID-19 samples.

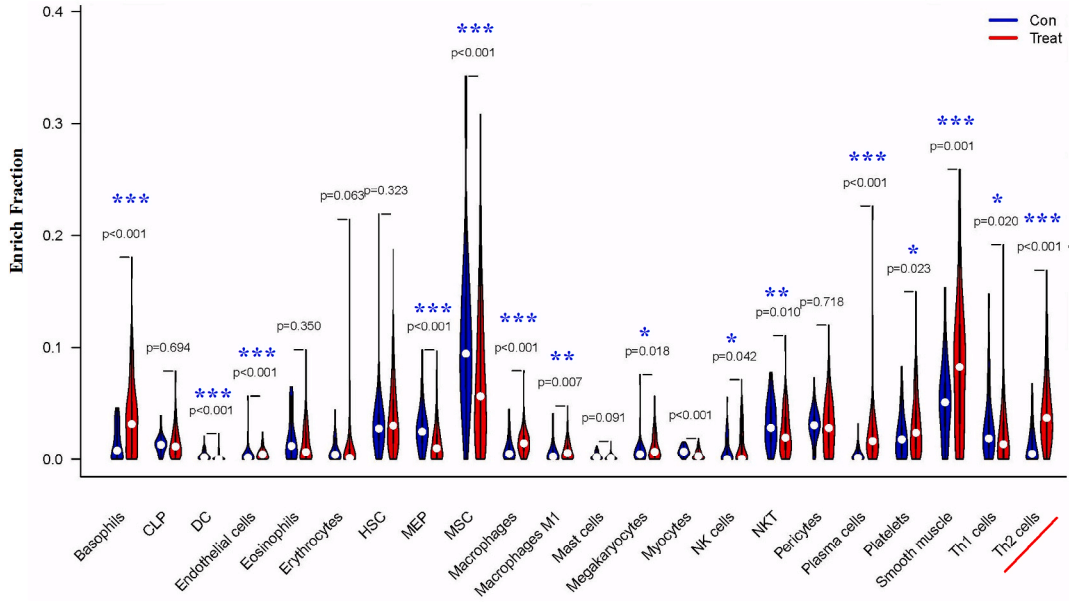

Fig. 2. The Immune-Enumeration Level in COVID-19 by X-cell algorithm.
$^{*}p < 0.05$, $^{**}p < 0.01$,$^{***}p < 0.01$, Con (control) *vs.* Treat (COVID-19) group.

were studied as important genes. Among them, the blue module contained 621 genes, the pink module contained 178 genes, the purple module contained 133 genes, the tan module contained 76 genes, the turquoise module contained 899 genes, and a total of 1907 genes. They were intersected with 1275 DEGs, and a total of 648 shared genes are obtained (Supplementary Fig. S1).

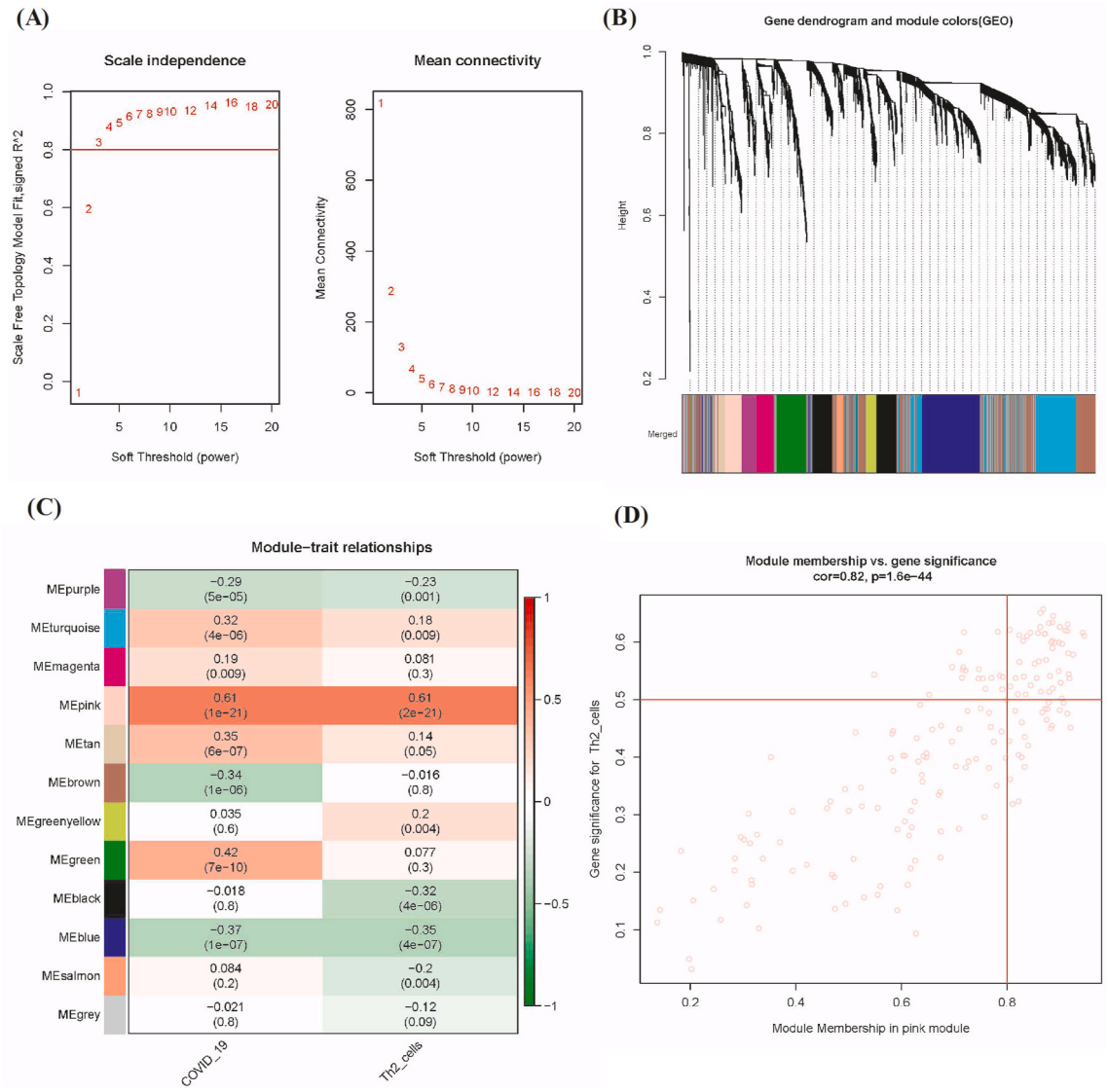

Fig. 3. Weighted gene co-expression network analysis (WGCNA).
(A) Soft-thresholding powers analysis. Estimation of the scale independence index and determination of the mean connectivity of the 1–20 soft threshold power (β = 0.8). It can be seen from the figure that when power = 4, the network meets the requirements of scale-free distribution. Therefore, the threshold β in this paper equal to 4. (B) Gene dendrogram and module colors. Different colors represent different gene modules, and grey modules are composed of genes that do not belong to any module. Each row and column represented a module and the genes of the module. This diagram showed the degree of correlation within the module. (C) Module-trait relationship. The rows in the figure correspond to consensus modules, and the columns correspond to macrophage subtypes. The numbers in each module indicated the correlation coefficients to show the association between the corresponding module and COVID-19 and Th2 cell, along with the p values shown below in parentheses (red indicates a positive correlation and green indicates a negative correlation). (D) Correlation between module membership and gene significance of gene in pink module. Scatter plots of modules eigengenes in the pink module.

3.5. GO and KEGG analysis of shared genes

In order to clarify the role of shared genes in biological processes and signal pathways, we performed GO and KEGG enrichment analysis. GO function enrichment analysis was carried out with the help of David database. The GO terms of the first 21 biological processes with FDR (false discovery rate) < 0.01 were arranged in Fig. 4A according to the enrichment fraction (-logFDR). The most important BP terms were closely related to the changes of cell state or activities after virus infection, such as organelle fission, nuclear division, chromosome segregation, mitotic nuclear division, sister chromatid segregation, and other cellular reactions. CC terms were mainly in the areas of cellular metabolism such as chromosomal region, secretory granule lumen, condensed chromosome, chromosome, and centromeric region. MF terms mainly involved carbohydrate binding, peroxidase activity, and oxidoreductase activity. The virus manipulates the host cell cycle to maximize its own replication. Most viral infections, including SARS-Cov-2 infection, induce cell G2/M phase arrest, cause cell cycle disorder and change cell cycle related factors to promote virus proliferation and replication [51,52]. In order to meet the needs of rapid cell proliferation, virus promote cells to carry out a series of metabolic stress reactions, such as increasing mitochondrial activity, carbohydrate synthesis, oxidation and peroxidation. SARS-CoV-2 activates mitochondria in immune cells, control mitochondrial activity, and provides favorable conditions for virus replication in mitochondrial structure [53]. SARS-CoV-2 infection leads to mitochondrial dysfunction and enhanced oxidative stress response [54].

For KEGG pathway enrichment analysis, the top 20 important pathways with FDR <0.01 were arranged according to enrichment fraction (-log FDR), as shown in Fig. 4B. The most significant enrichment

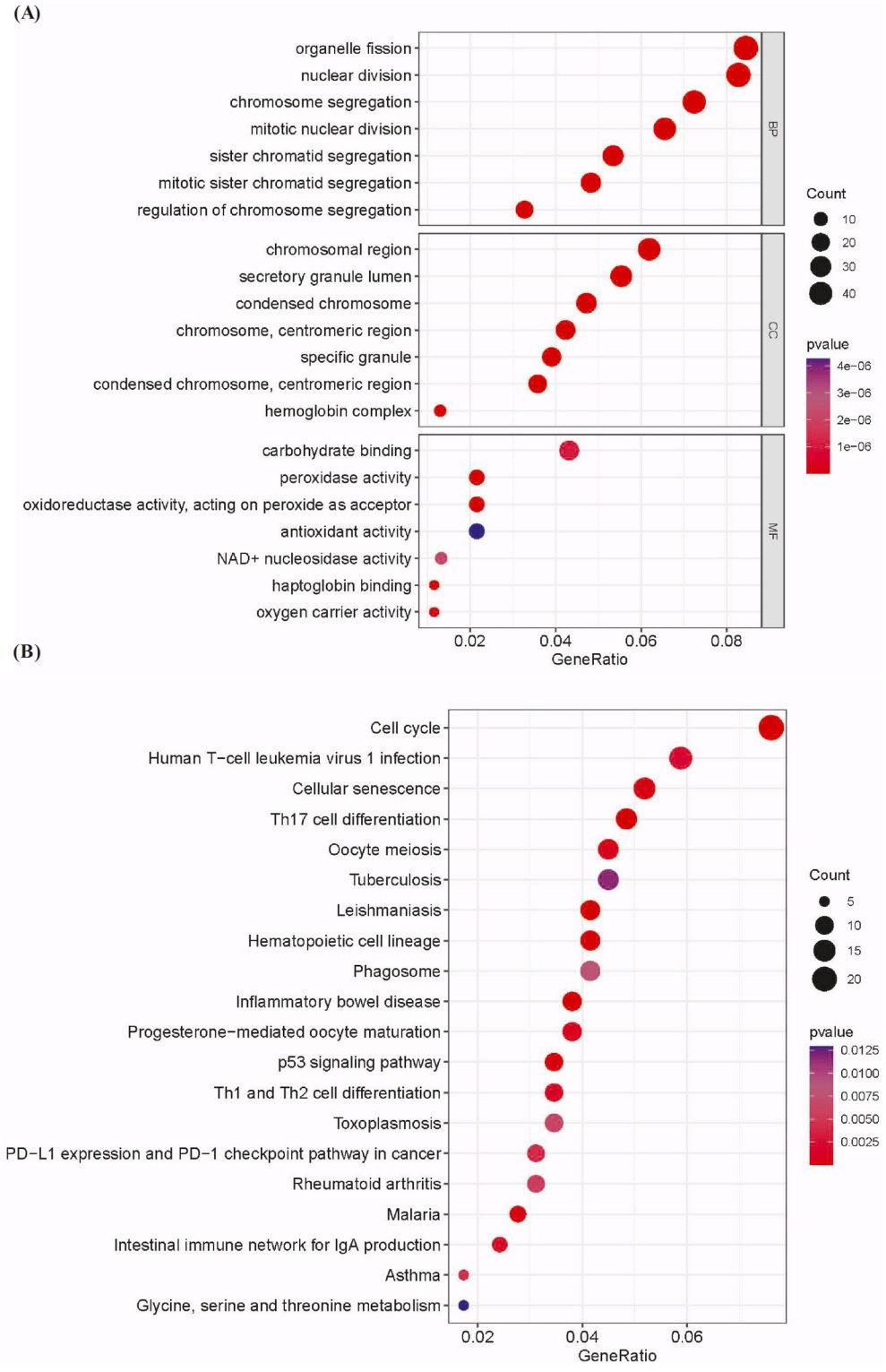

Fig. 4. Gene ontology (GO) and KEGG pathway analysis of shared genes.
(A) GO analysis. GO analysis divided into three functional groups: biological process (BP), cellular component (CC), and molecular function (MF). (B) KEGG pathway analysis. The circle represent count of genes associated with relative pathways.

pathway were related to the host's response to virus infection. Similar to the key points of GO analysis, most pathways were related to the cell cycle of virus infection, such as cell proliferation, division, and apoptosis. It mainly involved human T-cell leukemia virus 1 infection, progesterone-mediated oocyte matching, p53 signaling pathway, and oocyte meiosis. In addition, it was also related to the state of immune response after virus infection, such as Th17 cell differentiation, tuberculosis, leishmaniasis, hematopoietic cell lineage, inflammatory bowel disease, and toxoplasmosis. Such as tuberculosis, leishmaniasis, and toxoplasmosis are opportunistic infections in human immunodeficiency virus 1 (HIV-1) patients [55]. Most viral infections, including SARS-CoV infection, may lead to immunosuppression and cell proliferation

inhibition [56]. During viral infection, both innate and adaptive immune responses were activated [57]. The IL-6, TNF-α, IFN-β, IL-8, IL-1α/β, CCL2, MMP9 and MMP2 have been confirmed to be closely related to the pathogenesis of COVID-19 [58]. The severity of COVID-19 was positively correlated with the level of pro-inflammatory cytokines associated with Th17 cells [59]. The increase of TP53 expression leads to the induction of PBMC apoptosis, which reduced the frequency of apoptosis in COVID-19 patients [60]. In particular, the infection of SARS-CoV-2 leads to abnormal Th1 and Th2 cell differentiation responses (Supplementary Fig. S2).

In a word, the results of GO and KEGG analysis were related to the host's response to viral infection, including cell cycle activity, metabolic regulation, oxidative stress, cell proliferation and apoptosis, inflammatory process and immune response [61].

3.6. Identification of hub genes and validatetion of key genes

PPI is a reliable tool for assessing protein function in networks and identifying hub proteins in disease regulation [62]. To investigate the interaction of shared genes, an initial PPI network was created using STRING 11.0 [44]. The interaction scoring threshold was set to >0.990 (very high confidence level). Removes unconnected nodes from the network. The original PPI network consisted of 206 edges and 647 nodes (Fig. 5).

The cytoHubba plugin in cytoscape was used to perform hub genes analysis on PPI networks [45]. Based on the MCC algorithm, 20 hub genes were identified, including BUB1B, CCNB2, ESPL1, CCNA2, DLGAP5, PLK1, CDC20, CDCA8, TTK, TOP2A, PBK, BUB1, NCAPG, CDK1, UBE2C, NUSAP1, KIF11, TPX2, and AURKB (Fig. 6A). The expression of these hub genes increased and were more than twice that of the control group (logFC >0.5) (Fig. 6B). The hub genes were involved in many important cellular biological processes related to the proliferation and replication of virus infection, such as cell cycle activity, cell proliferation, cell mitosis, cell differentiation, apoptosis, cell metabolism, oxidative stress glycolysis and so on.

In order to find and confirm the key genes related to COVID-19 and Th2 cells, the expression levels of 20 hub genes were detected in discovery set (GSE157103 and GSE152641) and validation set (GSE171110,GSE152418, and GSE179627). In the validation set, we found that only the gene expression levels of CCNB1 (cyclin B1), BUB1 (budding uninhibited by benzimidazoles 1), and UBE2C (ubiquitin-conjugating enzyme E2C) were up-regulated in COVID-19 group, and there were statistically significant difference compared with the control group (Fig. 7A–C). The results were consistent with those in the discovery set (Supplementary Figs. S3A–C). Then, we performed ROC analysis to verify the diagnostic significance of three key genes (Fig. 7D and Supplementary Fig. S3D). The ROC values were generally between 0.5 and 1.0. The larger the value, the higher the accuracy of the model judgment, that is, the closer it is to 1, the better. In the discovery set, the AUC (area under the curve) values of the three key genes were greater than 0.8, and the AUC values were between 0.877 and 0.917 (Supplementary Fig. S3D). In the validation set, the AUC values of the three key genes were greater than 0.7, and the AUC values were between 0.708 and 0.998 (Fig. 7D). It can be seen that these three key genes were predicted with high accuracy in five datasets.

Finally, we also evaluated the correlation between the expression levels of three key genes and the risk of COVID-19 severity. We found a significant correlation between the gene expression levels of three key genes and the severity of COVID-19 ($p < 0.01$) (Supplementary Fig. S4).

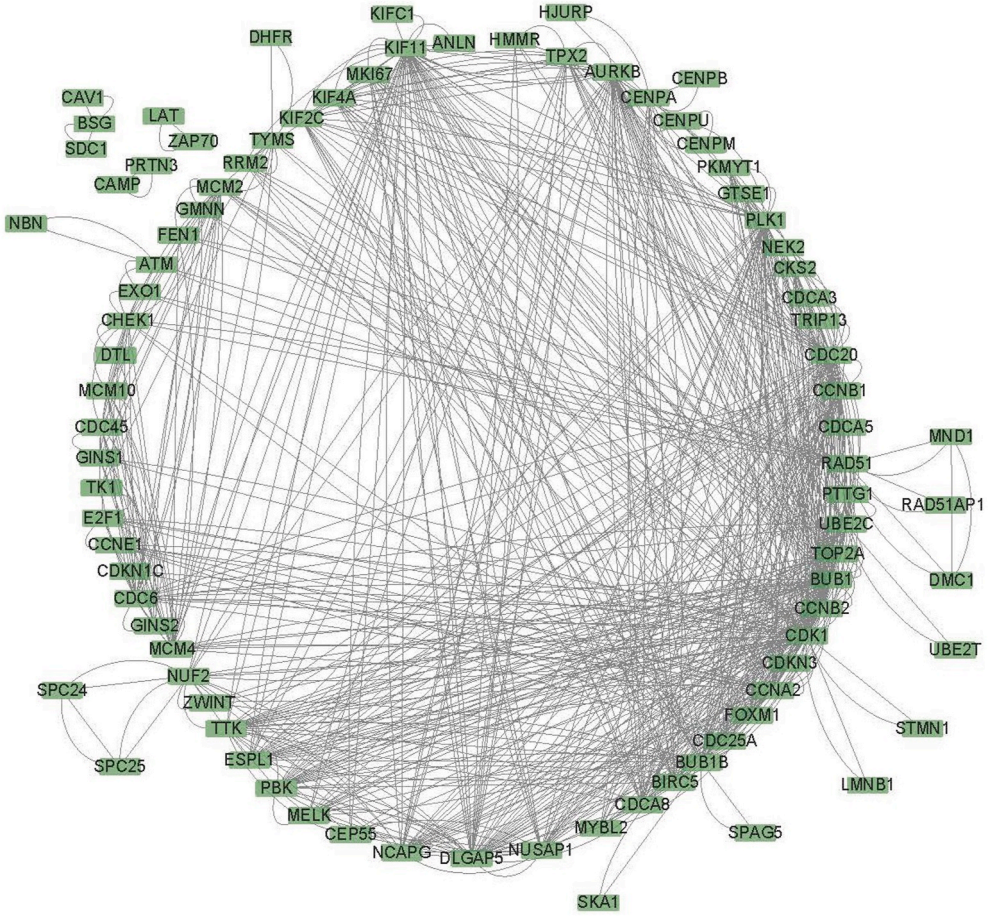

Fig. 5. Protein–protein interaction (PPI) network of shared genes was constructed using the STRING database.

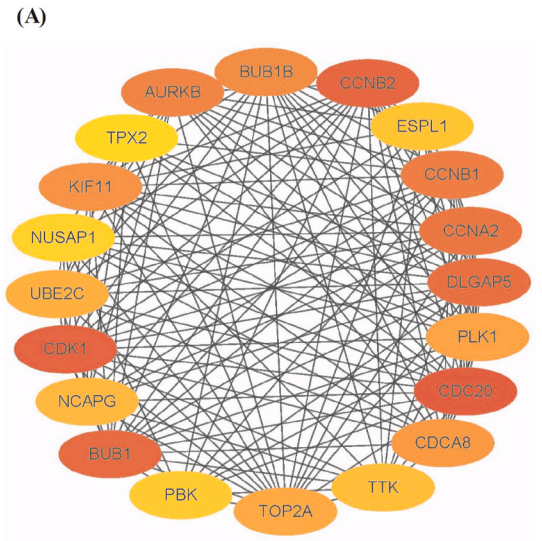

(B)

Gene Symbol	logFC	AveExpr	FDR
CDC20	1.187019963	3.531055295	6.30×10^{-14}
CDK1	1.584924523	3.500298364	1.94×10^{-21}
CCNB2	1.326625625	3.566673838	3.44×10^{-19}
BUB1	1.285790185	3.890048493	2.37×10^{-20}
DLGAP5	1.168602774	3.448465094	7.27×10^{-19}
CCNB2	1.326625625	3.566673838	3.44×10^{-19}
CCNB1	1.107825326	3.932803564	2.53×10^{-20}
AURKB	1.020881202	3.307827712	4.17×10^{-11}
BUB1B	0.949055119	3.082801836	1.81×10^{-18}
KIF11	0.926620648	3.896807495	3.24×10^{-18}
CDCA8	0.800976145	3.303719468	2.17×10^{-12}
PLK1	0.906765666	3.207796121	1.04×10^{-16}
TOP2A	1.318676774	4.145539508	6.30×10^{-24}
UBE2C	1.141537193	4.051835842	6.87×10^{-17}
NCAPG2	0.535016199	3.965485079	9.18×10^{-10}
TTK	0.863258691	2.58970366	1.48×10^{-14}
ESPL1	0.66579109	2.338111075	3.00×10^{-10}
PBK	1.313874758	1.966846175	$1.81\times10^{0-18}$
NUSAP1	0.751996501	2.786259936	1.95×10^{-06}
TPX2	1.149305767	3.775444847	8.35×10^{-21}

Fig. 6. Cytoscape analysis (cytoHubb) identified 20 genes are hub nodes in the network.
(A). Twenty hub genes identification by MCC algorithms. (B). Average gene expression (AveExpr) and logFC differential values *vs. control group.*

3.7. Screening potential therapeutic agents for COVID-19

Screening compounds that likely down-regulate the expression of three key genes using cMAP database (Supplementary Table S2). As shown in Table 2, the eleven small molecules or drugs with the highest absolute FC values (|FC|≥ 0.4) were chosen, which indicated significant correlations with COVID-19. Tanespimycin, alvespimycin, geldanamycin, troglitazone, and estradiol can better down-regulate the gene expression of CCNB1. Trichostatin A showed the effect of down regulating BUB1 gene expression. In addition, digoxigenin, monorden, helveticoside, lanatoside C, tretinoin, troglitazone, geldanamycin, tanespimycin, and alvespimycin better regulated the expression of UBE2C gene. Of particular interest was that troglitazone, geldanamycin, tanespimycin, and alvespimycin down-regulate both CCNB1 and UBE2C gene expression levels.

3.8. Molecular docking analysis predicts the binding modes between potential drugs and three key targets

The top 3 vital proteins were chosen as viral proliferation and cell cycle regulation related proteins for molecular docking analysis, including CCNB1, BUB1, and UBE2C, all of which have been shown to be strongly associated with the pathogenesis of COVID-19 and SARS-Cov-2.11 drug candidates were identified that could down-regulate three key genes using the cMAP database. Thus, molecular docking was used to calculate the binding energy and evaluate binding favorability (Table 3). The docking results showed that the 11 candidate drugs were promising inhibitors for each of the selected targets with moderate to strong binding affinities (−6.5 ∼ −18.8 kcal/mol). It was shown in the literature that the free binding energy was greater than −5.5 kcal/mol, indicating that the compound was in an inactive state [63]. The best results were obtained for the CCNB1-helveticoside, BUB1-helveticoside, and UBE2C-helveticoside complexes, with free binding energies of −16.0 kcal/mol, −18.8 kcal/mol, and −12.5 kcal/mol, respectively. It can be seen that helveticoside has good interaction with CCNB1,BUB1, and UBE2C. The optimal binding modes of each studied targets and drugs complex (bold shown in Table 3) were demonstrated in Fig. 8. For CCNB1-helveticoside complexes, hydrogen bonds between helveticoside and LEU83, ILE10, and LYS33 along with hydrophobic contacts between helveticoside and PHE82, ASP146, PHE80, ALA31, LEU135, and VAL64, significantly contributed to the stability of the complex (Fig. 8A). For complex BUB1-helveticoside, the hydrogen bonds between helveticoside with GLU795, LYS821, and TYR869, and hydrophobic bonds between helveticoside with ASP946, GLY796, ILE945, MET850, ILE924, GLY794, LEU868, VAL819, LEU793, and VAL801 further stabilized the structure of helveticoside (Fig. 8B). For UBE2C-helveticoside complexes, hydrogen bonds (ASP108 and CYS102), and hydrophobic contacts (GLY111, ASN149, PRO101, PHE98, LEU99, THR109, and TYR103) formed between protein residues and helveticoside contributed to stability of the complex and were clearly illustrated in Fig. 8C.

4. Discussion

COVID-19 is raging around the world, causing hundreds of millions of infections and millions of deaths [35]. The SARS-Cov-2 strain continuously mutates, rapidly increasing infection prevalence. Although there are several vaccines and anti-viral drugs, the virus continues to spread [64]. Developing potential therapies requires understanding the molecular basis for disease as well as the interaction between host and pathogen [9]. Identification of key disease genes and pathways will provide a foundation for drug target and biomarker development.

In this study, we used bioinformatics and systems biology methods to clarify the COVID-19 molecular regulatory mechanism. We used two COVID-19 data sets from the GEO database (GSE157103 and GSE152641) as the discovery set with which to analyze DEGs between COVID-19 and control samples. Then, WGCNA analysis was performed and a module comprised of genes closely related to COVID-19 and Th2 cell enrichment was constructed. A total of five statistically significant module genes with high correlation (purple, blue, pink, tan, and turquoise) were intersected with DEGs for a total of 648 shared genes. GO and KEGG analysis of shared genes showed that they were enriched for cell proliferation, differentiation, apoptosis, host inflammation, and immune response after virus infection. One of the most abundant enrichment pathways was the regulation of virus life cycle. These genes play a wide range of roles in the life cycle of SARS-CoV-2 infection such as promoting survival, attachment, entry, and replication of virus particles [65]. Next, STRING database was used to identify shared genes for construction of a PPI network. CytoHubba was used to identify the top 20 hub genes. Validation sets (GSE171110, GSE152418, and GSE179627) were used to verify the expression of these 20 key genes during COVID-19 infection. Only CCNB1, BUB1, and UBE2C genes were up-regulated in COVID-19 samples of the discovery and validation set,

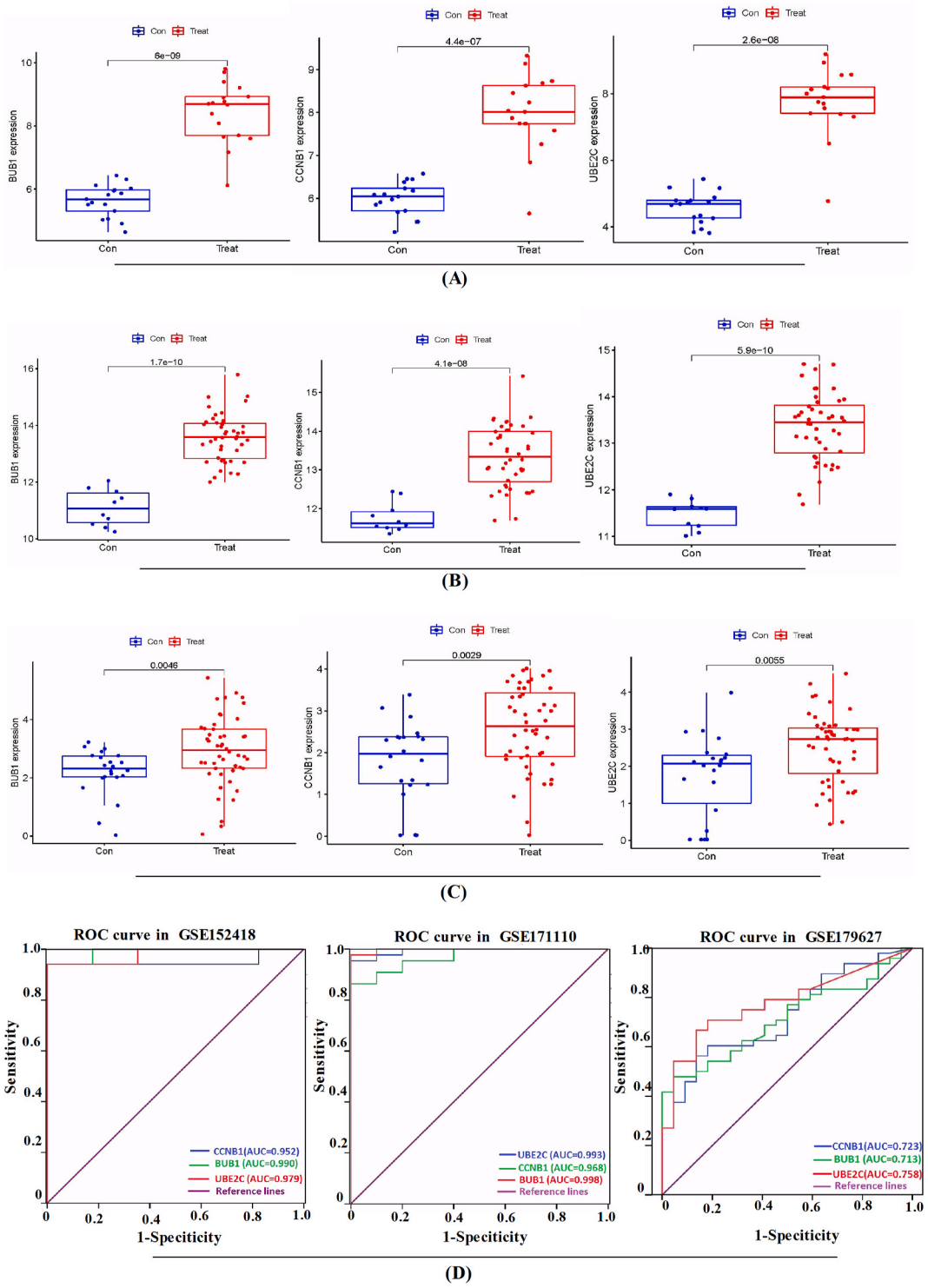

Fig. 7. Identification and validation of the diagnostic values of the key genes in GSE15241(A), GSE171110 (B), and GSE179627 (C)
(A)–(C) Differential expression of three key genes between the Treat (COVID-19) group and Con (control) group. (D) ROC curves for BUB1,CCNB1, and UBE2C gene in Validation set.

with statistically significant differences from the control group ($p <$ 0.05–0.001). ROC curve analysis showed that the AUCs of the three genes in the discovery and validation set were greater than 0.70, indicating good diagnostic capability. In addition, the expression levels of the three genes were significantly correlated with the severity of COVID-19. Therefore, CCNB1, BUB1, and UBE2C likely play a key role in the progression of COVID-19 and were identified as key genes that were potential therapeutic targets for COVID-19. We also found 11 small molecules that down-regulated the expression of these three key genes, which may be potential drugs for COVID-19.

The three key genes CCNB1, BUB1, and UBE2C are directly involved in cell cycle regulation. In eukaryotic cells, cells grow and divide in a gradual manner, a process known as the cell cycle. It can be divided into several different stages, GAP 1 (G1), synthesis (S), GAP 2 (G2) and mitosis (M), followed by cytoplasmic division [66]. Viruses are specialized intracellular parasites whose survival depends on their

Table 2
Small molecules or drugs with down-regulation mRNA expression of four key genes in cMAP database (|Fold Change| >0.4).

Drug Name	Gene Name	Molecular Formula	Fold Change	Description
Trichostatin A	BUB1	$C_{29}H_{40}N_2O_9$	−0.476829	A benzoquinone antineoplastic antibiotic isolated from the bacterium Streptomyces hygroscopicus. It has a role as an antiviral agent, an antineoplastic agent, an antimicrobial agent, a cysteine protease inhibitor and a Hsp90 inhibitor.
Tanespimycin	CCNB1	$C_{31}H_{43}N_3O_8$	−0.983234	Tanespimycin is a benzoquinone antineoplastic antibiotic derived from the antineoplastic antibiotic geldanamycin. It is a potent inhibitor of heat shock protein 90 (Hsp90)
Alvespimycin		$C_{32}H_{48}N_4O_8$	−0.525979	Alvespimycin is an analogue of the antineoplastic benzoquinone antibiotic geldanamycin. It has a role as a Hsp90 inhibitor.
Geldanamycin		$C_{29}H_{40}N_2O_9$	−0.759691	A benzoquinone antineoplastic antibiotic isolated from the bacterium Streptomyces hygroscopicus. It has a role as an antiviral agent, an antineoplastic agent, an antimicrobial agent, a cysteine protease inhibitor and a Hsp90 inhibitor.
Troglitazone		$C_{24}H_{27}NO_5S$	−0.592884	Troglitazone was the first thiazolidinedione approved for use in the United States and was licensed for use in type 2 diabetes. It has a role as a hypoglycemic agent, an antioxidant, a vasodilator agent, an anticonvulsant, an anticoagulant, a platelet aggregation inhibitor, an antineoplastic agent
Estradiol		$C_{18}H_{24}O_2$	−0.422529	Therapeutic Estradiol is a synthetic form of estradiol, a steroid sex hormone vital to the maintenance of fertility and secondary sexual characteristics in females, that may be used as hormone replacement therapy. It may play a role in immune and inflammatory processes.
Digoxigenin	UBE2C	$C_{23}H_{34}O_5$	−1.14604	Digoxigenin is a hydroxy steroid that consists of 5 beta-cardanolide having a double bond at the 20 (22)-position as well as hydroxy groups at the 3 beta-, 12 beta- and 14 beta-positions. It has been isolated from the plant species of the genus Digitalis.
Monorden		$C_{18}H_{17}ClO_6$	−0.566037	Monorden is an antifungal macrolactone antibiotic, obtained from Diheterospora chlamydosporia and Chaetomium chiversii that inhibits protein tyrosine kinase and heat shock protein 90 (Hsp90). It has a role as a tyrosine kinase inhibitor, an antifungal agent and a metabolite.
Helveticoside		$C_{29}H_{42}O_9$	−1.00438	Helveticoside is a cardenolide glycoside.
Lanatoside C		$C_{49}H_{76}O_{20}$	−0.879748	Cedilanid
Tretinoin		$C_{20}H_{28}O_2$	−0.609428	Tretinoin is a naturally-occurring acid of retinol. Tretinoin binds to and activates retinoic acid receptors (RARs), thereby inducing changes in gene expression that lead to cell differentiation, decreased cell proliferation, and inhibition of tumorigenesis.
Troglitazone		ditto	−0.407626	Ditto
Geldanamycin		ditto	−0.736052	Ditto
Tanespimycin		ditto	−0.534826	Ditto
Alvespimycin		ditto	−0.712526	Ditto

Table 3
Docking score for the binding free energy of the ligand to the targets.

Name of compounds (ligands)	PubChem CID	Binding free energy of the targets (kcal•mol^{-1})		
		CCNB1	BUB1	UBE2C
Trichostatin A	444,732	−8.2	−8.6	−7.2
Tanespimycin	6505803	−8.2	−6.9	−6.5
Alvespimycin	5288674	−9.2	−8.5	−9.0
Geldanamycin	5288382	−10.8	−9.6	−8.3
Troglitazone	5591	−9.0	−8.4	−7.2
Estradiol	5757	−9.6	−9.9	−7.7
Digoxigenin	15,478	−11.2	−13.2	−8.8
Monorden	6323491	−11.8	−12.6	−9.5
Helveticoside	441,860	**−16.0**	**−18.8**	**−12.5**
Lanatoside C	656,630	−12.3	−13.4	−10.0
Tretinoin	444,795	−11.6	−13.6	−8.5

ability to replicate in living organisms, with the virus interacting with each phase of the eukaryotic cell cycle [51]. Many viruses promote their own replication by interacting with host factors that regulate cell cycle processes [67]. For example, HIV-1, infectious bronchitis virus (IBV),

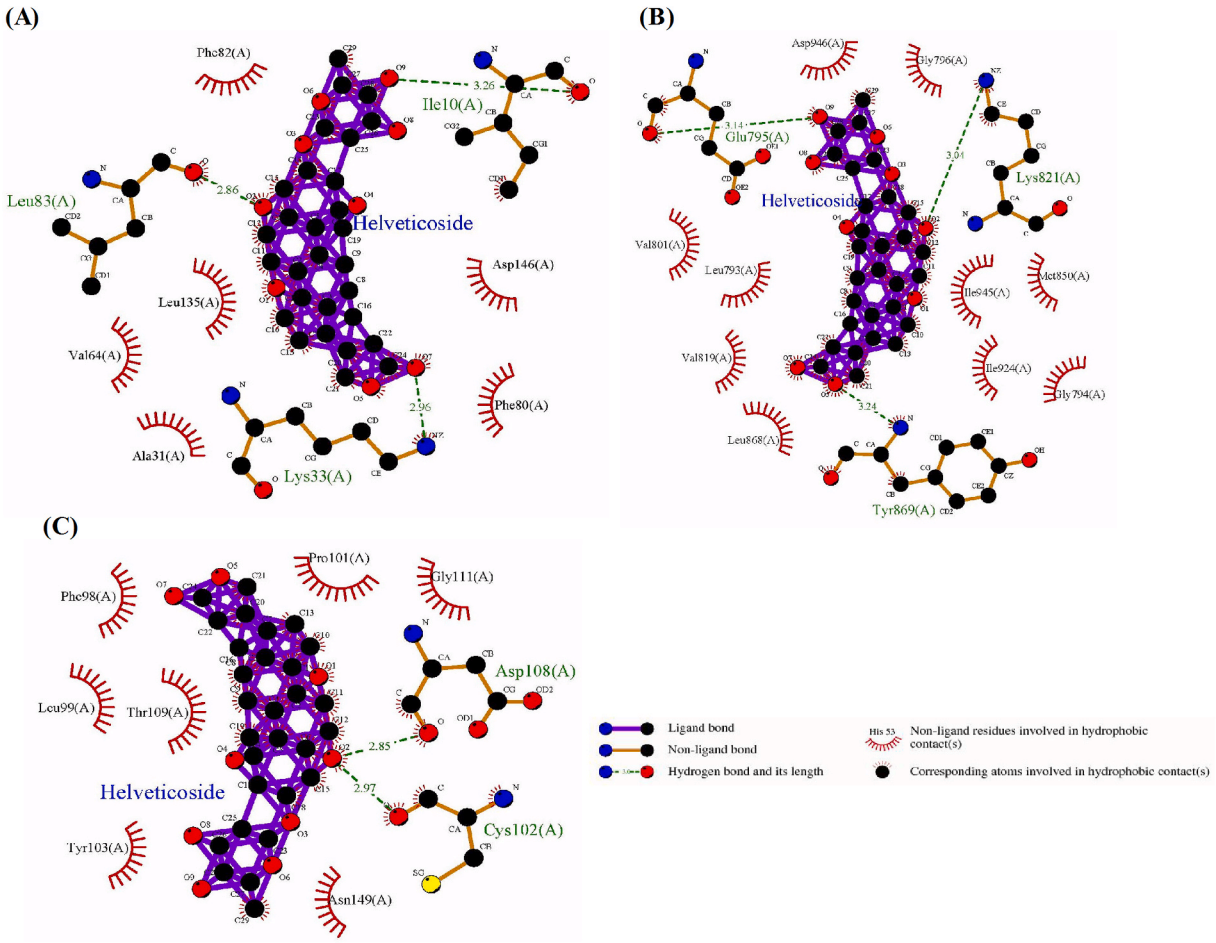

Fig. 8. Interaction between CCNB1,BUB1, UBE2C and helveticoside.
Interaction of (A) CCNB1, (B) BUB1, and (C) UBE2C with helveticoside is shown. Hydrogen bonds were shown as dotted lines (green).

and SARS-CoV manipulate the host cell cycle, block cells in the G0/G1 phase and thus provide favorable conditions for virus production [68–70]. CCNB1 proteins are a family of cell cycle proteins with serine/threonine kinase activity that are involved in the regulation of the G2/M cell cycle transition [71]. CCNB1 plays a role in proliferation, apoptosis, and the transformation of epithelial cells into mesenchymal cells [72]. CCNB1 also regulates signal transduction by CD8 + T cells [73]. BUB1 is a member of the BUB family and the mitotic arrest-deficient (MAD) protein family, which plays an important role in chromosome segregation [74]. Aberrant expression of BUB1 affects the function of the spindle checkpoint, resulting in chromosomal instability during mitosis. BUB1 also plays an important role in virus entry [75]. UBE2C is a member of the E2 family of ubiquitin-conjugating enzymes that plays an important role in cellular regulation by specifically binding to late cell cycle facilitation complexes. UBE2C participates in the ubiquitin protein degradation pathway [76]. As an important post-translational protein modification, ubiquitination is involved in cell cycle regulation, apoptosis, DNA repair, transcriptional regulation, autophagy, and other important intracellular reactions. Ubiquitination is important for cell renewal of intracellular proteins, removal of senescent proteins, and maintenance of cellular internal stability [77]. UBE2C is required for the disruption of mitotic cyclins and securin, which are essential to spindle assembly checkpoint and mitotic exit [78]. Various disruptions of the cell cycle caused by pathogens are attributed to alterations in cell cycle progression as well as changes in the expression of cell cycle-related proteins. CCNB1, BUB1, and UBE2C are highly expressed during COVID-19 infection, suggesting that SARS-CoV-2 can cause interference of host cell cycle genes, and manipulate these genes to accelerate virus replication and progression. Thus, the identified three hub genes may represent key genes for COVID-19 and therapeutic candidate targets [65].

In order to prevent the invasion of various pathogens, CD4 + helper T cells play an important role through cellular and humoral regulation. Helper T cells can be divided into two categories, Th1 and Th2, based on cytokine production. Th1 cells mainly secrete interferon-γ (IFN-γ), IL-2, IL-18, TNF-α, and granulocyte-macrophage colony-stimulating factor (GM-CSF) and mediate the cellular immune response. Th2 cells secrete IL-4, IL-5, IL-10, IL-6, and IL-13 and mediate humoral immunity [79]. Both Th1 and Th2 cells produce IL-3, IFN-γ, and GM-CSF. Th1 and Th2 cytokines are thought to be regulators of tissue injury and fibrosis [80]. Under normal physiological conditions, Th1 and Th2 cells are in a dynamic balance, which maintains normal host cellular and humoral immunity [81,82]. SARS-CoV-2 infection increases the secretion of Th2 cytokines (e.g. IL-13 and IL-4) into plasma [2]. A Th2/Th1 imbalance has been associated with COVID-19 progression and inflammatory mediator levels including GM-CSF, IL-1α/β, TNF-α, IFN-β, IL-8, and IL-6 are significantly increased in response to SARS-CoV-2 [36,83–85]. Increased serum levels of IL-6 and IL-8 predict severity of COVID-19 pneumonia and patient prognosis [86], which indicating that SARS-Cov-2 induces a massive secretion of cytokines produced by Th2 cells. SARS-CoV-2 replication is dependent upon cell cycle genes that are related to cellular proliferation. This process simultaneously activates cell cycle protein-dependent kinase (Cdk)-bound kinase and related signaling pathways, such as mitogen-activated protein kinase (MAPK), mTOR, p53, nuclear factor (NF)-κB, and NOD-like receptors (NLR). These signaling pathways induce an inflammatory response, including

IL-1β, IL-6, and TNF-α produced by Th2 cells [87–90]. For instance, CCNB1 activates the PI3K/Akt signaling pathway and is involved in regulation of various cellular responses including $CD8^+$ T cell-related signaling [73,91]. BUB1 is required for efficient TGF-β signaling [92]. SARS-CoV-2 infection induces apoptosis of dendritic cells and activates the mTOR signaling pathway to polarize Th1 and Th2 cells by regulating the secretion of IL-6, IL-8, IL-10, IFN-γ, and IL-12 [93]. During the primary host response to SARS-CoV-2 infection, activation of casein kinase II (CK2) and p38 MAPK signaling pathways results in significant cellular effects such as phosphorylation of host and viral proteins, pro-inflammatory cytokine production, cytoskeletal remodeling, and the shutdown of mitotic kinases, which results in cell cycle arrest and promotion of viral replication [94–96]. NLRs are a specific class of cytoplasmic PRRs that regulate NF-κB signaling, pro-inflammatory cytokine production (e.g. IL-1β), and cell death [97]. SARS-CoV-2 activates the NOD-like receptor signaling pathway during proliferation and replication. This pathway and its members are important targets for cytokine storm reduction in patients with severe COVID-19 [98–100]. Activation of associated kinases and related signaling pathways results in the production of large quantities of Th2 cytokines, which support SARS-CoV-2 replication and inflammatory responses [101–103]. In brief, SARS-CoV-2 activates key cell cycle regulatory genes CCNB1, BUB1, and UBE2C in immune cells during infection, providing for favorable control of cell cycle gene activity and advantageous conditions for viral replication in immune cells [53]. Therefore, inhibition of these three cell cycle genes can control SARS-Cov-2 replication and excessive inflammation [104].

This study also used the cAMP database to identify 11 small molecules or drugs that may be effective against SARS-Cov-2, by targeting the three key genes. Trichostatin A (TSA) is a histone deacetylase (HDAC) inhibitor that induces acetylation of cytoplasmic NF-κB p65, which activates NF-κB and induces cell cycle arrest at G1, inhibiting cell growth and the proliferation of virus-infected cells [105]. Inhibition of Bub1-H2A interactions by H2A-K119 malonylation reduces BUB1-dependent H2A-S121 phosphorylation and crosstalk between lysine malonylation and serine/threonine phosphorylation, which may fine-tune chromatin function (e.g. chromosome segregation) [106]. TSA reduces histone acetylation levels and significantly limits respiratory syncytial virus (RSV) replication by upregulating the IFN-γ-related signaling pathway and inhibits RSV-induced release of pro-inflammatory cytokines (e.g. IL-6 and IL-8) and the production of oxidative stress-related molecules (e.g. malondialdehyde and nitric oxide) [107]. In this study, TSA was found to down-regulate the expression of BUB1. Therefore, TSA may inhibit SARS-Cov-2 replication and Th2 cell induced inflammatory factor production through cell cycle control and inhibition of immune cell-associated kinase signaling pathways.

Tanespimycin is a heat shock protein 90 (Hsp90) inhibitor. Hsp90 is a unique cellular chaperone whose primary function is to induce the post-translational maturation of a proprietary subset of transcription factors, kinases, and steroid hormone receptors. Some viruses use cellular Hsp90 for the folding and assembly of viral structural proteins and the maturation of viral enzymes. Tanespimycin controls latent HIV reactivation and prevents HIV gene expression by inhibiting NF-κB activation [108]. Further, tanespimycin interacts with DNA-dependent protein kinase (DNA-PK), protein kinase CK2, and inducible polypeptides (EIPs) [109]. Hsp90 plays an important role in the SARS-CoV-2 life cycle. EIPs (ATP6V0C or vATPase) are essential for viral entry and are involved in cell proliferation and differentiation [110]. *In vitro* studies have shown tanespimycin to efficiently inhibit the proliferation and replication of SARS-CoV-2 [109,110]. In this study, tanespimycin was found to down-regulate the cell cycle regulatory genes CCNB1 and UBE2C, which may inhibit the replication of SARS-CoV-2 and overproduction of cytokines through inhibition of the cell cycle as Hsp90 inhibitor.

Geldanamycin (GA), monorden, and alvespimycin are also Hsp90 inhibitors [111]. Alvespimycin is also an analogue of GA. GA binds to the ADP/ATP binding site of Hsp90, blocking the chaperone function of Hsp90, resulting in the rapid degradation of Hsp90-related client proteins via the ubiquitin-proteasome pathway [112]. Hsp90 is important for the replication of many viruses including HBV, HCV, HCMV, HSV, rhinovirus, and Ebola virus [113]. GA interrupts the replication of the above-mentioned viruses in cell culture systems. In an HSV-1 mouse encephalitis model, GA significantly reduced mouse mortality and increased the average number of mouse survival days [114]. Interestingly, studies have suggested that geldanamycin, and its analogues can be useful in combating the progression of SARS-CoV-2 [115]. Cytokine storms in viral infections are associated with the activation of pro-inflammatory mediators, including NF-κB and the mitogen-activated protein (MAP) kinase. Activation of NF-κB requires the stability and function of IκB kinase (IKK), which complexes with Hsp90. Thus, by interacting with Hsp90, GA can inhibit IKK and disrupt the activation of the NF-κB pathway. A recent study was conducted to examine the effect of HSP90 inhibitors on SARS-CoV-2 based on *in vitro* models and proposed this group as potent antiviral and anti-inflammatory agents [116]. In this study, GA, monorden, and alvespimycin were found to regulate the cell cycle genes CCNB1 or UBE2C. This regulation may inhibit the replication of SARS-Cov-2 and the overproduction of cytokines through the inhibition of the cell cycle, as well as cellular proliferation, apoptosis, and related kinase activity (similar to the principle of Hsp90 inhibitor).

Troglitazone is a peroxisome proliferator-activated receptor gamma (PPARgamma) agonist. PPARgamma, a member of the nuclear hormone receptor superfamily, is involved in the regulation of immune and inflammatory processes [117]. Troglitazone activate PPARgamma to inhibit the release of TNF-α from RSV infected A549 cells in a dose-dependent manner. Troglitazone also inhibits the release of GM-CSF, IL-1α, IL-6, and the chemokines CXCL8 (IL-8) and CCL5 (RANTES) [118]. The SARS-CoV-2 genome contains several non-structural proteins (NSPs), with NSP9 encoding a replicase essential for viral replication within the host. Studies have shown that troglitazone have a high affinity for NSP9 [119]. Troglitazone also blocks HBV post-adherence, i.e. the internalization of HBV preS 1 and its receptor taurocholate co-transporting polypeptide (NTCP) [120]. In this study, troglitazone was found to down-regulate the cell cycle regulatory genes, CCNB1 and UBE2C, inhibiting the replication of SARS-CoV-2 in host cells and overproduction of inflammatory factors.

Estradiol is a steroid sex hormone. The SARS-CoV2 Spike (S) protein has a potential estrogen binding site [121]. Men develop more severe COVID-19 than do women [122]. SARS-CoV-2 infected macrophages express ACE2 and produce elevated levels of IL-6, resulting in inflammation and a cytokine storm with overproduction of IL-1β, IL-2, IL-6, IL-8, and TNF-α [123,124]. Estradiol regulates the function of immune cells. Therefore the antiviral state of these cells can be altered by hormonal stimulation [125]. Estradiol also inhibits NF-κB mediated macrophage activation via miR-125 b and polarizes Th2 through regulation of B lymphocyte function [122,126]. As such, estrogen may be a potential therapeutic target for promotion of cellular resistance to SARS-CoV-2 [127]. Estradiol was found to inhibit viral entry by targeting the six-helix (6-HB) fusion core of SARS-CoV-2 S protein [128]. Estradiol also showed a strong improvement regarding fatality in COVID-19 [129]. Estrogen, interacting with ESR1/2 receptors, is an essential sex factor that protects COVID-19 patients from death by inhibiting inflammation and immune response caused by SARS-CoV-2 infection [130]. In this study, estradiol was found to have a down-regulatory effect on CCNB1, which may inhibit the replication of SARS-CoV-2 in host cells and overproduction of Th2 cell induced cytokines by control of the cell cycle.

Digoxigenin and lanatoside C are cardiac glycosides that may block the binding between host ACE2 and the S protein of SARS-CoV-2, preventing viral penetration into target cells [131]. Computer docking sites for digoxigenin and lanatoside C have been identified for the ACE2

receptor protein and the major protease, M^{pro} [132,133]. Digoxigenin effectively blocks the entry of SARS-CoV-2 Spike pseudotypes into human lung cells and also blocks the infectivity of natural SARS-CoV-2. Digoxigenin inhibition of TNF-α induced NF-κB signaling results from the reduced interaction of the pro-inflammatory TNFα/TNFR1 complex with the TNFα-associated death domain (TRADD) protein [134–136]. Lanatoside C is an effective inhibitor of the early stages of the dengue virus replication cycle and has broad-spectrum antiviral activity against dengue virus, Kunjin flavivirus, Chikungunya A virus and human enterovirus 71 [137]. Studies showed that cardiac medications (e.g. digitoxin) can block penetration by SARSCoV- 2 Spike-pseudotyped virus into human lung cells, and infectivity by native SARS-CoV-2 [131] and have the anti-viral properties [138]. In this study, digoxigenin and lanatoside C were found to down-regulate UBE2C, which may early inhibit the replication cycle of SARS-CoV-2 and the release of inflammatory cytokines.

Helveticoside is a cardenolide glycoside. Na +/K+ expressing-ATPase is the cellular receptor for cardenolides. Helveticoside reduces the expression of infectious gastroenteritis virus (TGEV) nucleocapsid and stinging protein and blocks TGEV infection-induced apoptosis and cytopathic effects [139]. Cardenolide exerts antiviral activities by binding to membrane sodium/potassium pump Na+/K + -ATPase [140]. The direct binding of cardenolides to Na+/K + -ATPase induces endocytosis, reduces Na+/K + -ATPase on the cell surface, disrupts cytosol homeostasis, and increases intracellular calcium [141–143]. In this study, helveticoside was found to has a strongly down-regulatory effect on UBE2C, which may inhibit the proliferation and apoptosis of SARS-CoV-2 in host cells, exerting an antiviral activity.

Tretinoin is a naturally-occurring acid of retinol. Tretinoin binds to and activates retinoic acid receptors (RARs), which modulates gene expression, induces cell differentiation, decreases cell proliferation, and inhibits tumorigenesis. Coronaviruses encodes an envelope (E) protein and a viral pore protein with ion channel activity that is essential for coronavirus assembly and pathophysiology. Tretinoin blocks the channel and inhibits the function of the viral pore protein, E [144]. Further, tretinoin is an active metabolite of vitamin A (retinol) that regulates a number of important processes including development, differentiation, proliferation, and apoptosis in a classic and non-classic manner and is dependent on the RAR [145]. In this study, tretinoin was found to down-regulate UBE2C and to inhibit the proliferation, differentiation, and apoptosis of SARS-Cov-2 in host cells, which resulted in antiviral and anti-inflammatory effects.

In silico results indicated these eleven drugs with good potential to inhibit the function of CCNB1, BUB1, and UBE2C. Eleven drugs trichostatin A, tanespimycin, alvespimycin, geldanamycin, troglitazone, estradiol, digoxigenin, monorden, helveticoside, lanatoside C, and tretinoin were found to have highest binding affinities with the CCNB1, BUB1, and UBE2C. It could be inferred that these eleven drugs individually or in combinations may be used as potential inhibitors of CCNB1, BUB1, and UBE2C of SARS-CoV-2 after exploring their *in vivo* antiviral potential.

In conclusion, these 11 compounds mainly act on cell cycle regulatory genes and exert antiviral and anti-inflammatory effects by down-regulating the gene expression of BUB1, CCNB1 and UBE2C, and inhibiting proliferation, differentiation and apoptosis of virus-infected cells, kinase activation and inflammatory over-reaction. The three key genes could be considered as promising therapeutic targets for COVID-19. Eleven drugs were potential therapeutic agents for COVID-19. However, the current study has a number of limitations. As our study involved only retrospective analysis, the exact function of these key genes and predicted therapeutic agents need to be further investigated and validated *in vivo*, *in vitro* and *in clinic* studies.

5. Conclusion

BUB1, CCNB1 and UBE2C were identified key genes for COVID-19 and could be promising therapeutic targets. Eleven drug candidates that could down-regulate three key genes may be potential therapeutic agents for COVID-19.

Author contributions

Qiying Jin and Wanxi Li: GEO dataset analysis and original manuscript writing. Jinyuan Liu, Wendi Yu, and Maosen Zeng: helped to proofread the references, complete the data analysis. Peiping Xu: study design, supervision, and funding support. All authors contributed to the article and approved the submitted version.

Funding

This work was partly supported by a Natural Science Foundation of China grant (82141208).

Declaration of competing interest

The authors declare no conflict of interest.

Acknowledgments

We thank the authors of the GSE157103, GSE152641, GSE169687, GSE152418, and GSE179627 datasets for their contribution. We thank International Science Editing (Co. Clare, Ireland) for the language editorial assistance in the preparation of the manuscript.

Appendix A. Supplementary data

Supplementary data to this article can be found online at https://doi.org/10.1016/j.compbiomed.2022.106134.

References

[1] K.A. Overmyer, E. Shishkova, I.J. Miller, J. Balnis, M.N. Bernstein, T.M. Peters-Clarke, J.G. Meyer, Q.W. Quan, L.K. Muehlbauer, E.A. Trujillo, et al., Large-scale multi-omic analysis of COVID-19 severity, Cell Syst 12 (1) (2021) 23–+.
[2] C. Huang, Y. Wang, X. Li, Clinical features of patients infected with 2019 novel coronavirus in Wuhan, China (vol 395, pg 497, 2020), Lancet 395 (10223) (2020), 496-496.
[3] R.L. Gottlieb, C.E. Vaca, R. Paredes, J. Mera, B.J. Webb, G. Perez, G. Oguchi, P. Ryan, B.U. Nielsen, M. Brown, et al., Early remdesivir to prevent progression to severe covid-19 in outpatients, N. Engl. J. Med. 386 (4) (2022) 305–315.
[4] L.D. Saravolatz, S. Depcinski, M. Sharma, Molnupiravir and Nirmatrelvir-Ritonavir: Oral COVID Antiviral Drugs, Clinical infectious diseases : an official publication of the Infectious Diseases Society of America, 2022.
[5] A. Vitiello, F. Ferrara, V. Troiano, R. La Porta, COVID-19 vaccines and decreased transmission of SARS-CoV-2, Inflammopharmacology 29 (5) (2021) 1357–1360.
[6] A. Koirala, Y.J. Joo, A. Khatami, C. Chiu, P.N. Britton, Vaccines for COVID-19: the current state of play, Paediatr. Respir. Rev. 35 (2020) 43–49.
[7] Q. Liu, C.Y. Qin, M. Liu, J. Liu, Effectiveness and safety of SARS-CoV-2 vaccine in real-world studies: a systematic review and meta-analysis, Infect Dis Poverty 10 (1) (2021).
[8] H.K. Elsawah, M.A. Elsokary, M.S. Abdallah, A.H. ElShafie, Efficacy and safety of remdesivir in hospitalized Covid-19 patients: systematic review and meta-analysis including network meta-analysis, Rev. Med. Virol. 31 (4) (2021).
[9] P.S. Arunachalam, F. Wimmers, C.K.P. Mok, R.A.P.M. Perera, M. Scott, T. Hagan, N. Sigal, Y.P. Feng, L. Bristow, O.T.Y. Tsang, et al., Systems biological assessment of immunity to mild versus severe COVID-19 infection in humans, Science 369 (6508) (2020) 1210. -+.
[10] X.H. Ren, S.Q. Wang, X.L. Chen, X.Y. Wei, G.Y. Li, S.C. Ren, T.T. Zhang, X. Zhang, Z.W. Lu, Z.B. You, et al., Multiple expression assessments of ACE2 and TMPRSS2 SARS-CoV-2 entry molecules in the urinary tract and their associations with clinical manifestations of COVID-19, Infect. Drug Resist. 13 (2020) 3977–3990.
[11] Bernhauerova V, Lisowski B, Rezelj VV, Vignuzzi M: Mathematical modelling of SARS-CoV-2 infection of human and animal host cells reveals differences in the infection rates and delays in viral particle production by infected cells. J. Theor. Biol. 2021, 531.
[12] R. Jain, S. Ramaswamy, D. Harilal, M. Uddin, T. Loney, N. Nowotny, H. Alsuwaidi, R. Varghese, Z. Deesi, A. Alkhajeh, et al., Host transcriptomic profiling of COVID-19 patients with mild, moderate, and severe clinical outcomes, Comput Struct Biotec 19 (2021) 153–160.
[13] Z.Q. Cui, R. Bhandari, Q. Lei, M.Z. Lu, L. Zhang, M.M. Zhang, F.Y. Sun, L.J. Feng, S.S. Zhao, Identification and exploration of novel macrophage M2-related

biomarkers and potential therapeutic agents in endometriosis, Front. Mol. Biosci. 8 (2021).
[14] J. Tang, M.J. Mou, Y.X. Wang, Y.C. Luo, F. Zhu, MetaFS, Performance assessment of biomarker discovery in metaproteomics, Briefings Bioinf. 22 (3) (2021).
[15] Q.X. Yang, B. Li, J. Tang, X.J. Cui, Y.X. Wang, X.F. Li, J. Hu, Y.Z. Chen, W.W. Xue, Y. Lou, et al., Consistent gene signature of schizophrenia identified by a novel feature selection strategy from comprehensive sets of transcriptomic data, Briefings Bioinf. 21 (3) (2020) 1058–1068.
[16] A. Derakhshani, N. Hemmat, Z. Asadzadeh, M. Ghaseminia, M.A. Shadbad, G. Jadideslam, N. Silvestris, V. Racanelli, B. Baradaran, Arginase 1 (Arg 1) as an up-regulated gene in COVID-19 patients: a promising marker in COVID-19 immunopathy, J. Clin. Med. 10 (5) (2021).
[17] A. Hasankhani, A. Bahrami, N. Sheybani, B. Aria, B. Hemati, F. Fatehi, H. Ghaem Maghami Farahani, G. Javanmard, M. Rezaee, J.P. Kastelic, et al., Differential Co-expression network analysis reveals key hub-high traffic genes as potential therapeutic targets for COVID-19 pandemic, Front. Immunol. 12 (2021), 789317.
[18] J.K. Das, S. Roy, P.H. Guzzi, Analyzing host-viral interactome of SARS-CoV-2 for identifying vulnerable host proteins during COVID-19 pathogenesis, Infect. Genet. Evol. : journal of molecular epidemiology and evolutionary genetics in infectious diseases 93 (2021), 104921.
[19] A. Sarma, S.A. Christenson, A. Byrne, E. Mick, A.O. Pisco, C. DeVoe, T. Deiss, R. Ghale, B.S. Zha, A. Tsitsiklis, et al., Tracheal aspirate RNA sequencing identifies distinct immunological features of COVID-19 ARDS, Nat. Commun. 12 (1) (2021) 5152.
[20] Z. Daniloski, T.X. Jordan, H.H. Wessels, D.A. Hoagland, S. Kasela, M. Legut, S. Maniatis, E.P. Mimitou, L. Lu, E. Geller, et al., Identification of required host factors for SARS-CoV-2 infection in human cells, Cell 184 (1) (2021) 92–105 e116.
[21] N. Saheb Sharif-Askari, F. Saheb Sharif-Askari, B. Mdkhana, H.A. Hussain Alsayed, H. Alsafar, Z.F. Alrais, Q. Hamid, R. Halwani, Upregulation of oxidative stress gene markers during SARS-COV-2 viral infection, Free Radic. Biol. Med. 172 (2021) 688–698.
[22] R. Tiwari, A.R. Mishra, A. Gupta, D. Nayak, Structural similarity-based prediction of host factors associated with SARS-CoV-2 infection and pathogenesis, J. Biomol. Struct. Dynam. (2021) 1–12.
[23] L. Feng, Y.Y. Yin, C.H. Liu, K.R. Xu, Q.R. Li, J.R. Wu, R. Zeng, Proteome-wide data analysis reveals tissue-specific network associated with SARS-CoV-2 infection, J. Mol. Cell Biol. 12 (12) (2020) 946–957.
[24] J. Hadjadj, N. Yatim, L. Barnabei, A. Corneau, J. Boussier, N. Smith, H. Pere, B. Charbit, V. Bondet, C. Chenevier-Gobeaux, et al., Impaired type I interferon activity and inflammatory responses in severe COVID-19 patients, Science 369 (6504) (2020) 718–724.
[25] E. Wyler, K. Mosbauer, V. Franke, A. Diag, L.T. Gottula, R. Arsie, F. Klironomos, D. Koppstein, K. Honzke, S. Ayoub, et al., Transcriptomic profiling of SARS-CoV-2 infected human cell lines identifies HSP90 as target for COVID-19 therapy, iScience 24 (3) (2021), 102151.
[26] H. Wang, J. Zhang, Z. Lu, W. Dai, C. Ma, Y. Xiang, Y. Zhang, Identification of potential therapeutic targets and mechanisms of COVID-19 through network analysis and screening of chemicals and herbal ingredients, Briefings Bioinf. 23 (1) (2022).
[27] N. El-Hachem, E. Eid, G. Nemer, G. Dbaibo, O. Abbas, N. Rubeiz, S. Zeineldine, G. M. Matar, J.P. Bikorimana, R. Shammaa, et al., Integrative transcriptome analyses empower the anti-COVID-19 drug arsenal, iScience 23 (11) (2020), 101697.
[28] W.F. Leong, H.C. Tan, E.E. Ooi, D.R. Koh, V.T. Chow, Microarray and real-time RT-PCR analyses of differential human gene expression patterns induced by severe acute respiratory syndrome (SARS) coronavirus infection of Vero cells, Microb. Infect. 7 (2) (2005) 248–259.
[29] J. Guo, H. Yu, J. Yang, Y. Li, X. Zhang, K. Mei, S. Chi, S. Yuan, H. Liu, S. El-Ashram, et al., Weighted gene co-expression network analysis revealed host transcriptional response to H1N1 influenza A virus infection, J. Infect. 82 (3) (2021) e4–e7.
[30] P. Langfelder, S. Horvath, WGCNA: an R package for weighted correlation network analysis, BMC Bioinf. 9 (2008) 559.
[31] S. van Dam, U. Vosa, A. van der Graaf, L. Franke, J.P. de Magalhaes, Gene co-expression analysis for functional classification and gene-disease predictions, Briefings Bioinf. 19 (4) (2018) 575–592.
[32] J. Zhang, D. Lin, K. Li, X. Ding, L. Li, Y. Liu, D. Liu, J. Lin, X. Teng, Y. Li, et al., Transcriptome analysis of peripheral blood mononuclear cells reveals distinct immune response in asymptomatic and Re-detectable positive COVID-19 patients, Front. Immunol. 12 (2021), 716075.
[33] Z.Z. Wang, K. Li, A.R. Maskey, W.H. Huang, A.A. Toutov, N. Yang, K. Srivastava, J. Geliebter, R. Tiwari, M.S. Miao, et al., A small molecule compound berberine as an orally active therapeutic candidate against COVID-19 and SARS: a computational and mechanistic study, Faseb. J. 35 (4) (2021).
[34] F.A. Lagunas-Rangel, V. Chavez-Valencia, High IL-6/IFN-gamma ratio could be associated with severe disease in COVID-19 patients, J. Med. Virol. 92 (10) (2020) 1789–1790.
[35] D. Banji, S.S. Alqahtani, O.J.F. Banji, S. Machanchery, A. Shoaib, Calming the inflammatory storm in severe COVID-19 infections: role of biologics- A narrative review, Saudi Pharmaceut. J. 29 (3) (2021) 213–222.
[36] A.B. Pavel, J.W. Glickman, J.R. Michels, S. Kim-Schulze, R.L. Miller, E. Guttman-Yassky, Th2/Th1 cytokine imbalance is associated with higher COVID-19 risk mortality, Front. Genet. 12 (2021).
[37] H. Bozkaya, A.M. Bozdayi, A. Turkyilmaz, H. Cetinkaya, C. Yurdaydin, O. Uzunalimoglu, TH1/TH2 cytokines and their relations to HBeAg status and ALT flares in chronic HBV infection, Hepatology 28 (4) (1998), 721a-721a.
[38] D. Aran, Z.C. Hu, A.J. Butte, xCell: digitally portraying the tissue cellular heterogeneity landscape, Genome Biol. 18 (2017).
[39] M.E. Ritchie, B. Phipson, D. Wu, Y.F. Hu, C.W. Law, W. Shi, G.K. Smyth, Limma powers differential expression analyses for RNA-sequencing and microarray studies, Nucleic Acids Res. 43 (7) (2015).
[40] S.A. Thair, Y.D. He, Y. Hasin-Brumshtein, S. Sakaram, R. Pandya, J.Y. Toh, D. Rawling, M. Remmel, S. Coyle, G.N. Dalekos, et al., Transcriptomic similarities and differences in host response between SARS-CoV-2 and other viral infections, iScience 24 (1) (2021).
[41] D.C. Bu, H.T. Luo, P.P. Huo, Z.H. Wang, S. Zhang, Z.H. He, Y. Wu, L.H. Zhao, J. J. Liu, J.C. Guo, et al., KOBAS-i: intelligent prioritization and exploratory visualization of biological functions for gene enrichment analysis, Nucleic Acids Res. 49 (W1) (2021) W317–W325.
[42] da W. Huang, B.T. Sherman, R.A. Lempicki, Bioinformatics enrichment tools: paths toward the comprehensive functional analysis of large gene lists, Nucleic Acids Res. 37 (1) (2009) 1–13.
[43] D.W. Huang, B.T. Sherman, R.A. Lempicki, Systematic and integrative analysis of large gene lists using DAVID bioinformatics resources, Nat. Protoc. 4 (1) (2009) 44–57.
[44] D. Szklarczyk, A.L. Gable, D. Lyon, A. Junge, S. Wyder, J. Huerta-Cepas, M. Simonovic, N.T. Doncheva, J.H. Morris, P. Bork, et al., STRING v11: protein-protein association networks with increased coverage, supporting functional discovery in genome-wide experimental datasets, Nucleic Acids Res. 47 (D1) (2019) D607–D613.
[45] C.H. Chin, S.H. Chen, H.H. Wu, C.W. Ho, M.T. Ko, C.Y. Lin, cytoHubba: identifying hub objects and sub-networks from complex interactome, BMC Syst. Biol. 8 (2014).
[46] P. Shannon, A. Markiel, O. Ozier, N.S. Baliga, J.T. Wang, D. Ramage, N. Amin, B. Schwikowski, T. Ideker, Cytoscape: a software environment for integrated models of biomolecular interaction networks, Genome Res. 13 (11) (2003) 2498–2504.
[47] J. Lamb, E.D. Crawford, D. Peck, J.W. Modell, I.C. Blat, M.J. Wrobel, J. Lerner, J. P. Brunet, A. Subramanian, K.N. Ross, et al., The connectivity map: using gene-expression signatures to connect small molecules, genes, and disease, Science 313 (5795) (2006) 1929–1935.
[48] O. Trott, A.J. Olson, Software news and update AutoDock Vina: improving the speed and accuracy of docking with a new scoring function, efficient optimization, and multithreading, J. Comput. Chem. 31 (2) (2010) 455–461.
[49] M.F. Sanner, Python: a programming language for software integration and development, J. Mol. Graph. Model. 17 (1) (1999) 57–61.
[50] A.C. Wallace, R.A. Laskowski, J.M. Thornton, Ligplot - a program to generate schematic diagrams of protein ligand interactions, Protein Eng. 8 (2) (1995) 127–134.
[51] B. Dove, G. Brooks, K. Bicknell, T. Wurm, J.A. Hiscox, Cell cycle perturbations induced by infection with the coronavirus infectious bronchitis virus and their effect on virus replication, J. Virol. 80 (8) (2006) 4147–4156.
[52] S.M. Harrison, B.K. Dove, L. Rothwell, P. Kaiser, I. Tarpey, G. Brooks, J.A. Hiscox, Characterisation of cyclin D1 down-regulation in coronavirus infected cells, FEBS Lett. 581 (7) (2007) 1275–1286.
[53] K. Holder, P.H. Reddy, The COVID-19 effect on the immune system and mitochondrial dynamics in diabetes, obesity, and dementia, Neuroscientist 27 (4) (2021) 331–339.
[54] J. Saleh, C. Peyssonnaux, K.K. Singh, M. Edeas, Mitochondria and microbiota dysfunction in COVID-19 pathogenesis, Mitochondrion 54 (2020) 1–7.
[55] J.E. Gallant, R.D. Moore, R.E. Chaisson, Prophylaxis for opportunistic infections in patients with hiv-infection, Ann. Intern. Med. 120 (11) (1994) 932–944.
[56] T. Mizutani, S. Fukushi, D. Iizuka, O. Inanami, M. Kuwabara, H. Takashima, H. Yanagawa, M. Saijo, I. Kurane, S. Morikawa, Inhibition of cell proliferation by SARS-CoV infection in Vero E6 cells, FEMS Immunol. Med. Microbiol. 46 (2) (2006) 236–243.
[57] D.D. Chaplin, Overview of the immune response, J. Allergy Clin. Immunol. 125 (2) (2010) S3–S23.
[58] F. Coperchini, L. Chiovato, L. Croce, F. Magri, M. Rotondi, The cytokine storm in COVID-19: an overview of the involvement of the chemokine/chemokine-receptor system, Cytokine Growth Factor Rev. 53 (2020) 25–32.
[59] M. Lingeswaran, T. Goyal, R. Ghosh, S. Suri, P. Mitra, S. Misra, P. Sharma, Inflammation, immunity and immunogenetics in COVID-19: a narrative review, Indian J. Clin. Biochem. 35 (3) (2020) 260–273.
[60] Y. Xiong, Y. Liu, L. Cao, D.H. Wang, M. Guo, A. Jiang, D. Guo, W.J. Hu, J.Y. Yang, Z.D. Tang, et al., Transcriptomic characteristics of bronchoalveolar lavage fluid and peripheral blood mononuclear cells in COVID-19 patients, Emerg. Microb. Infect. 9 (1) (2020) 761–770.
[61] P. Asrani, M.I. Hassan, SARS-CoV-2 mediated lung inflammatory responses in host: targeting the cytokine storm for therapeutic interventions, Mol. Cell. Biochem. 476 (2) (2021) 675–687.
[62] S.I. Berger, R. Iyengar, Network analyses in systems pharmacology, Bioinformatics 25 (19) (2009) 2466–2472.
[63] P. Eleftheriou, D. Amanatidou, A. Petrou, A. Geronikaki, In silico evaluation of the effectivity of approved protease inhibitors against the main protease of the novel SARS-CoV-2 virus, Molecules 25 (11) (2020).
[64] J.C. Zhang, B. Xie, K. Hashimoto, Current status of potential therapeutic candidates for the COVID-19 crisis, Brain Behav. Immun. 87 (2020) 59–73.
[65] J. Gong, H. Dong, Q.S. Xia, Z.Y. Huang, D.K. Wang, Y. Zhao, W.H. Liu, S.H. Tu, M. M. Zhang, Q. Wang, et al., Correlation analysis between disease severity and inflammation-related parameters in patients with COVID-19: a retrospective study, BMC Infect. Dis. 20 (1) (2020).

[66] M.B. Mayhew, J.W. Robinson, B.Y. Jung, S.B. Haase, A.J. Hartemink, A generalized model for multi-marker analysis of cell cycle progression in synchrony experiments, Bioinformatics 27 (13) (2011) I295–I303.
[67] Y. Fan, S. Sanyal, R. Bruzzone, Breaking bad: how viruses subvert the cell cycle, Front. Cell. Infect. Microbiol. 8 (2018).
[68] Z.Y. Wang, T. Zhong, Y. Wang, F.M. Song, X.F. Yu, L.P. Xing, W.Y. Zhang, J.H. Yu, S.C. Hua, X.F. Yu, Human enterovirus 68 interferes with the host cell cycle to facilitate viral production, Front. Cell. Infect. Microbiol. 7 (2017).
[69] W.C. Goh, M.E. Rogel, C.M. Kinsey, S.F. Michael, P.N. Fultz, M.A. Nowak, B. H. Hahn, M. Emerman, HIV-1 Vpr increases viral expression by manipulation of the cell cycle: a mechanism for selection of Vpr in vivo, Nat. Med. 4 (1) (1998) 65–71.
[70] X.L. Yuan, J. Wu, Y.J. Shan, Z.Y. Yao, B. Dong, B. Chen, Z.H. Zhao, S.Q. Wang, J. P. Chen, Y.W. Cong, SARS coronavirus 7a protein blocks cell cycle progression at G0/G1 phase via the cyclin D3/pRb pathway, Virology 346 (1) (2006) 74–85.
[71] T. Miyazaki, S. Arai, Two distinct controls of mitotic Cdk1/Cyclin b1 activity requisite for cell growth prior to cell division, Cell Cycle 6 (12) (2007) 1419–1425.
[72] B. Li, H.B. Zhu, G.D. Song, J.H. Cheng, C.Z. Li, Y.Z. Zhang, P. Zhao, Regulating the CCNB1 gene can affect cell proliferation and apoptosis in pituitary adenomas and activate epithelial-to-mesenchymal transition, Oncol. Lett. 18 (5) (2019) 4651–4658.
[73] E.K. Kleczko, K.H. Marsh, L.C. Tyler, S.B. Furgeson, B.L. Bullock, C.J. Altmann, M. Miyazaki, Gitomer BY, Harris PC, Weiser-Evans MCM et al.: **CD8(+) T cells modulate autosomal dominant polycystic kidney disease progression**, Kidney Int. 94 (6) (2018) 1127–1140.
[74] A. Sarkar, D.A. Beard, B.R. Franza, Effect of binding in cyclic phosphorylation-dephosphorylation process and in energy transformation, Math. Biosci. 202 (1) (2006) 175–193.
[75] S. Yang, J.J. Yu, Z.Q. Fan, S.T. Gong, H. Tang, L. Pan, Bub1 facilitates virus entry through endocytosis in a model of Drosophila pathogenesis, J. Virol. 92 (18) (2018).
[76] L.F. Chang, Z.G. Zhang, J. Yang, S.H. McLaughlin, D. Barford, Atomic structure of the APC/C and its mechanism of protein ubiquitination, Nature 522 (7557) (2015) 450–+.
[77] Z.L. Hao, H. Zhang, J. Cowell, Ubiquitin-conjugating enzyme UBE2C: molecular biology, role in tumorigenesis, and potential as a biomarker, Tumor Biol. 33 (3) (2012) 723–730.
[78] C.L. Xie, C. Powell, M. Yao, J.M. Wu, Q.H. Dong, Ubiquitin-conjugating enzyme E2C: a potential cancer biomarker, Int. J. Biochem. Cell Biol. 47 (2014) 113–117.
[79] J.L. Gardell, D.C. Parker, Despite disorganized synapse structure, Th2 cells maintain directional delivery of CD40L to antigen-presenting B cells, PLoS One 12 (10) (2017).
[80] H. Mojiri-Forushani, A.A. Hemmati, A. Khodadadi, M. Rashno, Valsartan attenuates bleomycin-induced pulmonary fibrosis by inhibition of NF-kappa B expression and regulation of Th1/Th2 cytokines, Immunopharmacol. Immunotoxicol. 40 (3) (2018) 225–231.
[81] H. Chakir, H.P. Wang, D.E. Lefebvre, J. Webb, F.W. Scott, T-bet/GATA-3 ratio as a measure of the Th1/Th2 cytokine profile in mixed cell populations: predominant role of GATA-3, J. Immunol. Methods 278 (1–2) (2003) 157–169.
[82] L. Aoudjehane, G. Bisch, O. Scatton, C. Granier, J. Gaston, C. Housset, P. Roingeard, F.L. Cosset, F. Perdigao, P. Balladur, et al., Infection of human liver myofibroblasts by hepatitis C virus: a direct mechanism of liver fibrosis in hepatitis C, PLoS One 10 (7) (2015).
[83] T.A. Xie, M.Y. Han, X.R. Su, H.H. Li, J.C. Chen, X.G. Guo, Identification of Hub genes associated with infection of three lung cell lines by SARS-CoV-2 with integrated bioinformatics analysis, J. Cell Mol. Med. 24 (20) (2020) 12225–12230.
[84] N. Hemmat, A. Derakhshani, H. Bannazadeh Baghi, N. Silvestris, B. Baradaran, S. De Summa, Neutrophils, crucial, or harmful immune cells involved in coronavirus infection: a bioinformatics study, Front. Genet. 11 (2020) 641.
[85] F. Coperchini, L. Chiovato, L. Croce, F. Magri, M. Rotondi, The cytokine storm in COVID-19: an overview of the involvement of the chemokine/chemokine-receptor system, Cytokine Growth Factor Rev. 53 (2020) 25–32.
[86] B. Russell, C. Moss, G. George, A. Santaolalla, A. Cope, S. Papa, M. Van Hemelrijck, Associations between immune-suppressive and stimulating drugs and novel COVID-19-a systematic review of current evidence, Ecancermedicalscienc 14 (2020) 1–43.
[87] R. Patra, N.C. Das, S. Mukherjee, Targeting human TLRs to combat COVID-19: a solution? J. Med. Virol. 93 (2) (2021) 615–617.
[88] P. Conti, G. Ronconi, A. Caraffa, C.E. Gallenga, R. Ross, I. Frydas, S.K. Kritas, Induction of pro-inflammatory cytokines (IL-1 and IL-6) and lung inflammation by Coronavirus-19 (COVI-19 or SARS-CoV-2): anti-inflammatory strategies, J. Biol. Regul. Homeost. Agents 34 (2) (2020) 327–331.
[89] S.M. Harrison, B.K. Dove, L. Rothwell, P. Kaiser, I. Tarpey, G. Brooks, J.A. Hiscox, Characterisation of cyclin D1 down-regulation in coronavirus infected cells, FEBS Lett. 581 (7) (2007) 1275–1286.
[90] H. Mojiri-Forushani, A.A. Hemmati, A. Khodadadi, M. Rashno, Valsartan attenuates bleomycin-induced pulmonary fibrosis by inhibition of NF-kappaB expression and regulation of Th1/Th2 cytokines, Immunopharmacol. Immunotoxicol. 40 (3) (2018) 225–231.
[91] J. Gu, X. Liu, J. Li, Y. He, MicroRNA-144 inhibits cell proliferation, migration and invasion in human hepatocellular carcinoma by targeting CCNB1, Cancer Cell Int. 19 (2019) 15.
[92] S. Nyati, B.S. Gregg, J. Xu, G. Young, L. Kimmel, M.K. Nyati, D. Ray, C. Speers, A. Rehemtulla, TGFBR2 mediated phosphorylation of BUB1 at Ser-318 is required for transforming growth factor-beta signaling, Neoplasia 22 (4) (2020) 163–178.
[93] S. Morris, M.S. Swanson, A. Lieberman, M. Reed, Z.Y. Yue, D.M. Lindell, N. W. Lukacs, Autophagy-mediated dendritic cell activation is essential for innate cytokine production and APC function with respiratory syncytial virus responses, J. Immunol. 187 (8) (2011) 3953–3961.
[94] B.G.G. Pinto, A.E.R. Oliveira, Y. Singh, L. Jimenez, A.N.A. Goncalves, R.L. T. Ogava, R. Creighton, J.P.S. Peron, H.I. Nakaya, ACE2 expression is increased in the lungs of patients with comorbidities associated with severe COVID-19, J. Infect. Dis. 222 (4) (2020) 556–563.
[95] T. Mizutani, S. Fukushi, M. Saijo, I. Kurane, S. Morikawa, Phosphorylation of p38 MAPK and its downstream targets in SARS coronavirus-infected cells, Biochem Bioph Res Co 319 (4) (2004) 1228–1234.
[96] J. Kindrachuk, B. Ork, B.J. Hart, S. Mazur, M.R. Holbrook, M.B. Frieman, D. Traynor, R.F. Johnson, J. Dyall, J.H. Kuhn, et al., Antiviral potential of ERK/MAPK and PI3K/AKT/mTOR signaling modulation for Middle East respiratory syndrome coronavirus infection as identified by temporal kinome analysis, Antimicrob. Agents Chemother. 59 (2) (2015) 1088–1099.
[97] G. Chen, M.H. Shaw, Y.G. Kim, G. Nunez, NOD-like receptors: role in innate immunity and inflammatory disease, Annu Rev Pathol-Mech 4 (2009) 365–398.
[98] C.M. Sergi, B. Chiu, Targeting NLRP3 inflammasome in an animal model for coronavirus disease 2019 (COVID-19) caused by the severe acute respiratory syndrome coronavirus 2 (SARS-CoV-2), J. Med. Virol. 93 (2) (2021) 669–670.
[99] Q.W. Huang, X.M. Wu, X.Y. Zheng, S.H. Luo, S.W. Xu, J.P. Weng, Targeting inflammation and cytokine storm in COVID-19, Pharmacol. Res. (2020) 159.
[100] P. Krishnamoorthy, A.S. Raj, S. Roy, N.S. Kumar, H. Kumar, Comparative transcriptome analysis of SARS-CoV, MERS-CoV, and SARS-CoV-2 to identify potential pathways for drug repurposing, Comput. Biol. Med. (2021) 128.
[101] M.Z. Tay, C.M. Poh, L. Renia, P.A. MacAry, L.F.P. Ng, The trinity of COVID-19: immunity, inflammation and intervention, Nat. Rev. Immunol. 20 (6) (2020) 363–374.
[102] P. Icard, H. Lincet, Z.R. Wu, A. Coquerel, P. Forgez, M. Alifano, L. Fournel, The key role of Warburg effect in SARS-CoV-2 replication and associated inflammatory response, Biochimie 180 (2021) 169–177.
[103] N. Lodhi, R. Singh, S.P. Rajput, Q. Saquib, SARS-CoV-2: understanding the transcriptional regulation of ACE2 and TMPRSS2 and the role of single nucleotide polymorphism (SNP) at codon 72 of p53 in the innate immune response against virus infection, Int. J. Mol. Sci. 22 (16) (2021).
[104] X.J. Sun, T.Y. Wang, D.Y. Cai, Z.W. Hu, J.A. Chen, H. Liao, L.M. Zhi, H.X. Wei, Z. H. Zhang, Y.Y. Qiu, et al., Cytokine storm intervention in the early stages of COVID-19 pneumonia, Cytokine Growth Factor Rev. 53 (2020) 38–42.
[105] T. Katsura, S. Iwai, Y. Ota, H. Shimizu, K. Ikuta, Y. Yura, The effects of trichostatin A on the oncolytic ability of herpes simplex virus for oral squamous cell carcinoma cells, Cancer Gene Ther. 16 (3) (2009) 237–245.
[106] T. Ishiguro, K. Tanabe, Y. Kobayashi, S. Mizumoto, M. Kanai, S.A. Kawashima, Malonylation of histone H2A at lysine 119 inhibits Bub1-dependent H2A phosphorylation and chromosomal localization of shugoshin proteins, Sci Rep-Uk 8 (2018).
[107] Q.Q. Feng, Z.L. Su, S.Y. Song, H. Xu, B. Zhang, L. Yi, M. Tian, H.W. Wang, Histone deacetylase inhibitors suppress RSV infection and alleviate virus-induced airway inflammation, Int. J. Mol. Med. 38 (3) (2016) 812–822.
[108] P. Joshi, E. Maidji, C.A. Stoddart, Inhibition of heat shock protein 90 prevents HIV rebound, J. Biol. Chem. 291 (19) (2016) 10332–10346.
[109] T.H. Fatoki, O. Ibraheem, I.O. Ogunyemi, A.C. Akinmoladun, H.U. Ugboko, C. J. Adeseko, O.A. Awofisayo, S.J. Olusegun, J.M. Enibukun, Network analysis, sequence and structure dynamics of key proteins of coronavirus and human host, and molecular docking of selected phytochemicals of nine medicinal plants, J. Biomol. Struct. Dynam. 39 (16) (2021) 6195–6217.
[110] L. Han, K. Li, C.Z. Jin, J. Wang, Q.J. Li, Q.L. Zhang, Q.Y. Cheng, J. Yang, X.C. Bo, S.Q. Wang, Human enterovirus 71 protein interaction network prompts antiviral drug repositioning, Sci Rep-Uk 7 (2017).
[111] W. Basha, R. Kitagawa, M. Uhara, H. Imazu, K. Uechi, J. Tanaka, Geldanamycin, a potent and specific inhibitor of Hsp90, inhibits gene expression and replication of human cytomegalovirus, Antivir. Chem. Chemother. 16 (2) (2005) 135–146.
[112] J.H. Connor, M.O. McKenzie, G.D. Parks, D.S. Lyles, Antiviral activity and RNA polymerase degradation following Hsp90 inhibition in a range of negative strand viruses, Virology 362 (1) (2007) 109–119.
[113] D.R. Smith, S. McCarthy, A. Chrovian, G. Olinger, A. Stossel, T.W. Geisbert, L. E. Hensley, J.H. Connor, Inhibition of heat-shock protein 90 reduces Ebola virus replication, Antivir. Res. 87 (2) (2010) 187–194.
[114] Y.H. Li, Q.N. Lu, H.Q. Wang, P.Z. Tao, J.D. Jiang, Geldanamycin, a ligand of heat shock protein 90, inhibits herpes simplex virus type 2 replication both in vitro and in vivo, J. Antibiot. 65 (10) (2012) 509–512.
[115] J. Nahalka, Transcription of the envelope protein by 1-L protein-RNA recognition code leads to genes/proteins that are relevant to the SARS-CoV-2 life cycle and pathogenesis, Curr. Issues Mol. Biol. 44 (2) (2022) 791–816.
[116] E. Wyler, K. Mosbauer, V. Franke, A. Diag, L.T. Gottula, R. Arsie, F. Klironomos, D. Koppstein, K. Honzke, S. Ayoub, et al., Transcriptomic profiling of SARS-CoV-2 infected human cell lines identifies HSP90 as target for COVID-19 therapy, iScience 24 (3) (2021).
[117] R.A. Daynes, D.C. Jones, Emerging roles of PPARs in inflammation and immunity, Nat. Rev. Immunol. 2 (10) (2002) 748–759.
[118] R. Arnold, M. Neumann, W. Konig, Peroxisome proliferator-activated receptor-gamma agonists inhibit respiratory syncytial virus-induced expression of

intercellular adhesion molecule-1 in human lung epithelial cells, Immunology 121 (1) (2007) 71–81.
[119] A. Chandra, V. Gurjar, M.Z. Ahmed, A.S. Alqahtani, I. Qamar, N. Singh, Exploring potential inhibitor of SARS-CoV2 replicase from FDA approved drugs using insilico drug discovery methods, J. Biomol. Struct. Dynam. 40 (12) (2022) 5507–5514.
[120] K. Fukano, S. Tsukuda, M. Oshima, R. Suzuki, H. Aizaki, M. Ohki, S.Y. Park, M. Muramatsu, T. Wakita, C. Sureau, et al., Troglitazone impedes the oligomerization of sodium taurocholate cotransporting polypeptide and entry of hepatitis B virus into hepatocytes, Front. Microbiol. 9 (2019).
[121] A. Tomasovic, D. Stanzer, I.K. Svetec, M.S. Miklenic, SARS-CoV2 S protein features potential estrogen binding site, Food Technol. Biotechnol. 59 (1) (2021) 24–30.
[122] R.M.R. Lemes, A.J. Costa, C.S. Bartolomeo, T.B. Bassani, M.S. Nishino, G.J. D. Pereira, S.S. Smaili, R.M.D. Maciel, C.T. Braconi, E.F. da Cruz, et al., 17 beta-estradiol reduces SARS-CoV-2 infection in vitro, Phys. Rep. 9 (2) (2021).
[123] M.D. Park, Macrophages: a trojan horse in COVID-19? Nat. Rev. Immunol. 20 (6) (2020) 351.
[124] C. Qin, L. Zhou, Z. Hu, S. Zhang, S. Yang, Y. Tao, C. Xie, K. Ma, K. Shang, W. Wang, et al., Dysregulation of immune response in patients with coronavirus 2019 (COVID-19) in wuhan, China, Clin. Infect. Dis. : an official publication of the Infectious Diseases Society of America 71 (15) (2020) 762–768.
[125] A. Di Stadio, A. Della Volpe, M. Ralli, G. Ricci, Gender differences in COVID-19 infection. The estrogen effect on upper and lower airways. Can it help to figure out a treatment? Eur. Rev. Med. Pharmacol. Sci. 24 (10) (2020) 5195–5196.
[126] A.J. Murphy, P.M. Guyre, P.A. Pioli, Estradiol suppresses NF-kappa B activation through coordinated regulation of let-7a and miR-125b in primary human macrophages, J. Immunol. 184 (9) (2010) 5029–5037.
[127] A. Ramirez-de-Arellano, J. Gutierrez-Franco, E. Sierra-Diaz, A.L. Pereira-Suarez, The role of estradiol in the immune response against COVID-19, Horm-Int J Endocrino 20 (4) (2021) 657–667.
[128] C. Yang, X.Y. Pan, Y. Huang, C. Cheng, X.F. Xu, Y. Wu, Y.X. Xu, W.J. Shang, X. G. Niu, Y.H. Wan, et al., Drug repurposing of itraconazole and estradiol benzoate against COVID-19 by blocking SARS-CoV-2 Spike protein-mediated membrane fusion, Adv Ther-Germany 4 (5) (2021).
[129] U. Seeland, F. Coluzzi, M. Simmaco, C. Mura, P.E. Bourne, M. Heiland, R. Preissner, S. Preissner, Evidence for treatment with estradiol for women with SARS-CoV-2 infection, BMC Med. 18 (1) (2020).
[130] F.H. Li, A.C.M. Boon, A.P. Michelson, R.E. Foraker, M. Zhan, P.R.O. Payne, Estrogen hormone is an essential sex factor inhibiting inflammation and immune response in COVID-19, Sci Rep-Uk 12 (1) (2022).
[131] H. Caohuy, O. Eidelman, T.H. Chen, S.F. Liu, Q.F. Yang, A. Bera, N.I. Walton, T. T. Wang, H.B. Pollard, Common cardiac medications potently inhibit ACE2 binding to the SARS-CoV-2 Spike, and block virus penetration and infectivity in human lung cells, Sci Rep-Uk 11 (1) (2021).
[132] S. Ahmad, Y. Waheed, A. Abro, S.W. Abbasi, S. Ismail, Molecular screening of glycyrrhizin-based inhibitors against ACE2 host receptor of SARS-CoV-2, J. Mol. Model. 27 (7) (2021).
[133] I. Aanouz, A. Belhassan, K. El-Khatabi, T. Lakhlifi, M. El-Idrissi, M. Bouachrine, Moroccan Medicinal plants as inhibitors against SARS-CoV-2 main protease: computational investigations, J. Biomol. Struct. Dynam. 39 (8) (2021) 2971–2979.
[134] B.S. Pollard, J.C. Blanco, J.R. Pollard, Classical drug digitoxin inhibits influenza cytokine storm, with implications for covid-19 therapy, In Vivo 34 (6) (2020) 3723–3730.
[135] S.C. Miller, R.L. Huang, S. Sakamuru, S.J. Shukla, M.S. Attene-Ramos, P. Shinn, D. Van Leer, W. Leister, C.P. Austin, M.H. Xia, Identification of known drugs that act as inhibitors of NF-kappa B signaling and their mechanism of action, Biochem. Pharmacol. 79 (9) (2010) 1272–1280.
[136] Q.F. Yang, W. Huang, C. Jozwik, Y. Lin, M. Glasman, H. Caohuy, M. Srivastava, D. Esposito, W. Gillette, J. Hartley, et al., Cardiac glycosides inhibit TNF-alpha/NF-kappa B signaling by blocking recruitment of TNF receptor-associated death domain to the TNF receptor, P Natl Acad Sci USA 102 (27) (2005) 9631–9636.
[137] Y.Y. Cheung, K.C. Chen, H.X. Chen, E.K. Seng, J.J.H. Chu, Antiviral activity of lanatoside C against dengue virus infection, Antivir. Res. 111 (2014) 93–99.
[138] J. Cho, Y.J. Lee, J.H. Kim, S.I. Kim, S.S. Kim, B.S. Choi, J.H. Choi, Antiviral activity of digoxin and ouabain against SARS-CoV-2 infection and its implication for COVID-19, Sci Rep-Uk 10 (1) (2020).
[139] C.W. Yang, H.Y. Chang, H.Y. Hsu, Y.Z. Lee, H.S. Chang, I.S. Chen, S.J. Lee, Identification of anti-viral activity of the cardenolides, Na+/K+-ATPase inhibitors, against porcine transmissible gastroenteritis virus, Toxicol. Appl. Pharmacol. 332 (2017) 129–137.
[140] A.A. Agrawal, G. Petschenka, R.A. Bingham, M.G. Weber, S. Rasmann, Toxic cardenolides: chemical ecology and coevolution of specialized plant-herbivore interactions, New Phytol. 194 (1) (2012) 28–45.
[141] M. Diederich, F. Muller, C. Cerella, Cardiac glycosides: from molecular targets to immunogenic cell death, Biochem. Pharmacol. 125 (2017) 1–11.
[142] I. Prassas, E.P. Diamandis, Novel therapeutic applications of cardiac glycosides, Nat. Rev. Drug Discov. 7 (11) (2008) 926–935.
[143] C.W. Yang, H.Y. Chang, Y.Z. Lee, H.Y. Hsu, S.J. Lee, The cardenolide ouabain suppresses coronaviral replication via augmenting a Na(+)/K(+)-ATPase-dependent PI3K_PDK1 axis signaling, Toxicol. Appl. Pharmacol. 356 (2018) 90–97.
[144] D. Dey, S. Borkotoky, M. Banerjee, In silico identification of Tretinoin as a SARS-CoV-2 envelope (E) protein ion channel inhibitor, Comput. Biol. Med. (2020) 127.
[145] T. Okamura, M. Masuda, Y. Arai, C. Ishida, K. Shudou, H. Mizoguchi, All-trans retinoic acid modulates Fas antigen expression and affects cell proliferation and apoptosis in combination with anti-Fas monoclonal antibody in the human myeloma cell line, U266B1, Exp. Hematol. 26 (6) (1998) 501–506.